Virginia Center *for* Transportation
INNOVATION
& RESEARCH

Corrosion Assessment for the Failed Bridge Deck Closure Pour at Mile Marker 43 on I-81

http://www.virginiadot.org/vtrc/main/online_reports/pdf/14-r13.pdf

EBRAHIM K. ABBAS
Graduate Research Engineer

RICHARD E. WEYERS, Ph.D., P.E.
Professor

WILLIAM J. WRIGHT, Ph.D., P.E.
Associate Professor

C.L. ROBERTS-WOLLMANN, Ph.D., P.E.
Professor

Via Department of Civil and Environmental Engineering
Virginia Polytechnic Institute and State University

Final Report VCTIR 14-R13

VIRGINIA CENTER FOR TRANSPORTATION INNOVATION AND RESEARCH
530 Edgemont Road, Charlottesville, VA 22903-2454
www.VTRC.net

Standard Title Page - Report on Federally Funded Project

1. Report No.: FHWA/VCTIR 14-R13	2. Government Accession No.:	3. Recipient's Catalog No.:
4. Title and Subtitle: Corrosion Assessment for the Failed Bridge Deck Closure Pour at Mile Marker 43 on I-81		5. Report Date: April 2014 6. Performing Organization Code:
7. Author(s): Ebrahim K. Abbas, Richard E. Weyers, Ph.D., P.E., William J. Wright, Ph.D., P.E., and C.L. Roberts-Wollmann, Ph.D., P.E.		8. Performing Organization Report No.: VCTIR 14-R13
9. Performing Organization and Address: Virginia Tech Transportation Institute 3500 Transportation Research Plaza Blacksburg, VA 24061-0105		10. Work Unit No. (TRAIS): 11. Contract or Grant No.: 97825
12. Sponsoring Agencies' Name and Address: Virginia Department of Transportation 1401 E. Broad Street Richmond, VA 23219 Federal Highway Administration 400 North 8th Street, Room 750 Richmond, VA 23219-4825		13. Type of Report and Period Covered: Final Contract 14. Sponsoring Agency Code:
15. Supplementary Notes:		

16. Abstract:

Corrosion of reinforcing steel in concrete is a significant problem around the world. In the United States, there are approximately 600,000 bridges. Of those bridges, 24% are considered structurally deficient or functionally obsolete based on the December 2010 statistics from the Federal Highway Administration. The primary cause is chloride attack from deicing salts, which corrodes the reinforcing steel. Different solutions have been developed and used in practice to delay and prevent corrosion initiation.

The purpose of this research was to investigate the influence of corrosion and shrinkage on the failure mechanism that occurred on an I-81 bridge deck. After 17 years in service, a 3 ft by 3 ft closure pour section punched through. The closure was positioned under the left wheel path of the southbound right lane of the bridge deck. The bridge deck had been replaced in 1992 as part of a bridge rehabilitation project, and the reinforcement was epoxy coated. Four 4.5 ft by 10 ft slab sections, containing the closure, were saw cut from the deck, removed, and transported to the Virginia Tech Structures and Materials Research Laboratory for further evaluation. Also, for comparison, three new slabs were fabricated as part of the assessment program.

Corrosion evaluation and concrete shrinkage characterization were conducted in this study. The corrosion evaluation study included visual observation, clear concrete cover depth, concrete resistivity using single point resistivity, half-cell potential, and linear polarization using the 3LP device. Shrinkage was characterized on the lab cast slabs only. This consisted of monitoring shrinkage behavior of the specimens for 180 days and comparing of the data with five different shrinkage models. The joints of the lab cast specimens were monitored for cracking and leaking.

Based on the research results, it is recommended that similar joints be inspected for leaking and evidence of reinforcement corrosion every two years and all similar joints should be sealed to prevent leaking. In addition, it is recommended that construction joints in future decks built with staged construction use corrosion resistant reinforcement.

17 Key Words: Corrosion, reinforcement, decks, closure pours, failure		18. Distribution Statement: No restrictions. This document is available to the public through NTIS, Springfield, VA 22161.	
19. Security Classif. (of this report): Unclassified	20. Security Classif. (of this page): Unclassified	21. No. of Pages: 54	22. Price:

Form DOT F 1700.7 (8-72) Reproduction of completed page authorized

FINAL REPORT

CORROSION ASSESSMENT FOR THE FAILED BRIDGE DECK CLOSURE POUR AT MILE MARKER 43 ON I-81

Ebrahim K. Abbas
Graduate Research Engineer

Richard E. Weyers, Ph.D., P.E.
Professor

William J. Wright, Ph.D., P.E.
Associate Professor

C.L. Roberts-Wollmann, Ph.D., P.E.
Professor

Via Department of Civil and Environmental Engineering
Virginia Polytechnic Institute and State University

VCTIR Project Manager
Michael M. Sprinkel, P.E.
Virginia Center for Transportation Innovation and Research

In Cooperation with the U.S. Department of Transportation
Federal Highway Administration

Virginia Center for Transportation Innovation and Research
(A partnership of the Virginia Department of Transportation
and the University of Virginia since 1948)

Charlottesville, Virginia

April 2014
VTRC 14-R13

DISCLAIMER

The project that is the subject of this report was done under contract for the Virginia Department of Transportation, Virginia Center for Transportation Innovation and Research. The contents of this report reflect the views of the authors, who are responsible for the facts and the accuracy of the data presented herein. The contents do not necessarily reflect the official views or policies of the Virginia Department of Transportation, the Commonwealth Transportation Board, or the Federal Highway Administration. This report does not constitute a standard, specification, or regulation. Any inclusion of manufacturer names, trade names, or trademarks is for identification purposes only and is not to be considered an endorsement.

Each contract report is peer reviewed and accepted for publication by staff of Virginia Center for Transportation Innovation and Research with expertise in related technical areas. Final editing and proofreading of the report are performed by the contractor.

ABSTRACT

Corrosion of reinforcing steel in concrete is a significant problem around the world. In the United States, there are approximately 600,000 bridges. Of those bridges, 24% are considered structurally deficient or functionally obsolete based on the December 2010 statistics from the Federal Highway Administration. The primary cause is chloride attack from deicing salts, which corrodes the reinforcing steel. Different solutions have been developed and used in practice to delay and prevent corrosion initiation.

The purpose of this research was to investigate the influence of corrosion and shrinkage on the failure mechanism that occurred on an I-81 bridge deck. After 17 years in service, a 3 ft by 3 ft closure pour section punched through. The closure was positioned under the left wheel path of the southbound right lane of the bridge deck. The bridge deck had been replaced in 1992 as part of a bridge rehabilitation project, and the reinforcement was epoxy coated. Four 4.5 ft by 10 ft slab sections, containing the closure, were saw cut from the deck, removed, and transported to the Virginia Tech Structures and Materials Research Laboratory for further evaluation. Also, for comparison, three new slabs were fabricated as part of the assessment program.

Corrosion evaluation and concrete shrinkage characterization were conducted in this study. The corrosion evaluation study included visual observation, clear concrete cover depth, concrete resistivity using single point resistivity, half-cell potential, and linear polarization using the 3LP device. Shrinkage was characterized on the lab cast slabs only. This consisted of monitoring shrinkage behavior of the specimens for 180 days and comparing of the data with five different shrinkage models. The joints of the lab cast specimens were monitored for cracking and leaking.

Based on the research results, it is recommended that similar joints be inspected for leaking and evidence of reinforcement corrosion every two years and all similar joints should be sealed to prevent leaking. In addition, it is recommended that construction joints in future decks built with staged construction use corrosion resistant reinforcement.

FINAL REPORT

CORROSION ASSESSMENT FOR THE FAILED BRIDGE DECK CLOSURE POUR AT MILE MARKER 43 ON I-81

Ebrahim K. Abbas
Graduate Research Engineer

Richard E. Weyers, Ph.D., P.E.
Professor

William J. Wright, Ph.D., P.E.
Associate Professor

C.L. Roberts-Wollmann, Ph.D., P.E.
Professor

Via Department of Civil and Environmental Engineering
Virginia Polytechnic Institute and State University

INTRODUCTION

There are approximately 600,000 bridges in the United States according to the Federal Highway Administration (FHWA), and 24% (146,633 bridges) are considered structurally deficient or functionally obsolete based on the FHWA statistics dated December 2010 (FHWA, 2010). Most deficiencies are due to the corrosion of the reinforcing steel from deicing salt exposure. In the state of Virginia there are 10,403 bridges, and 33% (3,429 bridges) are considered structurally deficient or functionally obsolete, reflecting the amount of bridge repair and rehabilitation work required to maintain Virginia bridges. Typically, the first bridge component that needs to be repaired and rehabilitated is the concrete bridge deck, mainly due to a chloride-laden environment (deicing salts), which causes chloride-induced corrosion of the reinforcing steel imbedded in the concrete decks. The result is required rehabilitation before the concrete bridge decks reach their designed service life.

There are many methods used to delay premature rehabilitation work due to chloride induced corrosion of the reinforcing steel. Methods include decreasing the concrete permeability by decreasing the water to cement ratios (w/c), using cementitious materials (fly ash, slag, and silica fume), increasing the clear concrete cover depth for the reinforcing steel, using alternative types of reinforcing steel that have higher resistance to corrosion, using concrete surface sealers and membranes, and improving the deck drainage system. Concrete quality and cover depth are mainly influenced by construction method and procedures.

For chloride-induced corrosion of the reinforcing steel, an electrochemical process, the concrete void structure properties such as size, size distribution, connectivity, and degree of

saturation are controlling factors for the initiation of corrosion and the subsequent cracking and spalling of the cover concrete (Weyers et al., 2003).

Bridge decks with significant damage can be repaired with patching or overlays. In cases of extreme damage, deck replacement can be performed either by full or partial replacement depending on the severity of damage and other economic factors. Deck replacement requires a partial or full closure to traffic. Often staged construction is used to divert traffic to one half of the bridge, while the other side is demolished and replaced. After the two sides have been replaced, a closure pour is used to tie the halves together.

In 1992, several bridge decks on I-81 near Marion, Virginia, were replaced, using staged construction, as part of a bridge rehabilitation project. Figure 1 presents a transverse section showing the width and location of the closure pour. Epoxy-coated reinforcement (ECR) was used as the reinforcing steel. There was no formed keyway at the joint between the previously cast deck and the closure pour. After 17 years in service, a 3 ft by 3 ft closure pour section punched through, as shown in Figure 2. All of the bars along the closure/deck interface on both sides of the closure fractured.

The closure pour was positioned under the left wheel path of the southbound right lane of the bridge deck, so the joint was subject to a very large number of wheel loads. Observations at the bridge site indicated that the joint had opened slightly. In this case, it is possible that the reinforcing bars alone were carrying shear and moment across the joint. The open joint also provides a more direct path for deicing salts to penetrate to the reinforcing bars and induce corrosion. It is therefore likely that both fatigue and corrosion played a role in the failure of the closure.

PURPOSE AND SCOPE

The purpose of this study was to investigate the influence of corrosion and shrinkage on the failure mechanism that occurred on the I-81 bridge deck slab. Four 4.5 ft by 10 ft slab sections, containing the closure, were removed from the failed bridge deck to perform a series of tests. Those tests were performed to determine the corrosion severity. Three new slabs were fabricated in the lab, with the same design as the slabs removed from the actual bridge deck. This was done to understand the behavior and impact of shrinkage on the closure pour. Also, the lab cast slabs provide an undamaged baseline for comparison to the slabs removed from the bridge deck.

The testing was separated into two parts, corrosion evaluation and shrinkage characterization. Corrosion evaluation tests included visual observation, cover depth measurements, concrete resistivity using single point resistivity, half-cell potential, linear polarization using 3LP device. Shrinkage characteristics were evaluated on lab cast slabs only. Shrinkage specimens were monitored for 180 days and compared with predictive shrinkage model results. The joints were monitored to determine if cracks opened and allowed water leakage.

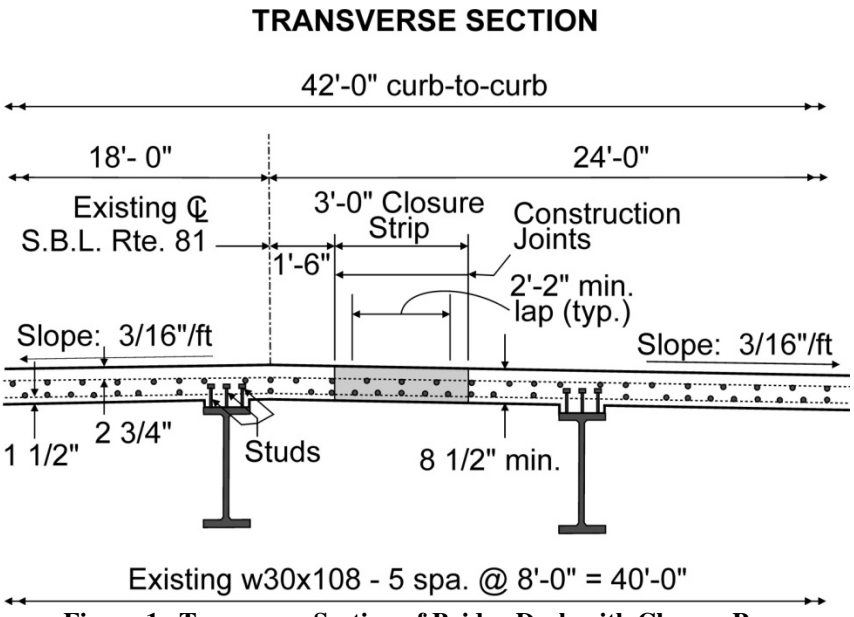

Figure 1. Transverse Section of Bridge Deck with Closure Pour

Figure 2. Failed Section of Closure Pour

METHODS

Specimens

The study was conducted on a total of eleven specimens, eight from the actual I-81 failed bridge and three new specimens fabricated and cast in the lab.

I-81 Deck Slabs

Sections measuring approximately 4.5 ft by 10 ft, deck were saw cut, removed from the bridge deck and delivered to the Thomas Murray Structures Laboratory at Virginia Tech. The sections contain the entire closure pour section along with approximately 9 in of the adjacent deck slab, as shown in Figure 3. There is a slight difference in the dimensions of the specimens due to construction and cutting precision, all slabs are shown in the Appendix.

Visual inspection was conducted on the field slabs in addition to corrosion readings, mechanical property testing, permeability characteristic testing, and density and saturation characteristic testing. After examining the sections, eight smaller pieces, 22 in wide, were cut from the four slabs to be used for fatigue and strength testing. The exact locations of the sections cut are also presented in the Appendix. The 22 in sections each contained two truss bars, and one each top and bottom straight reinforcing bars. These smaller specimens were also tested for strength and fatigue, and the results are presented elsewhere.

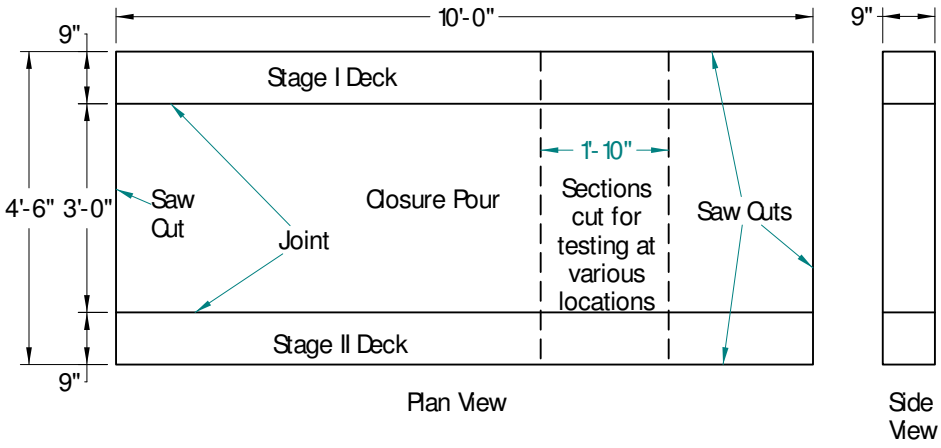

Figure 3. Approximate Dimensions of Slab Specimens

Lab Cast Specimens

Three slabs were fabricated and cast in the lab. The concrete used in casting the slabs was A-4 ready mixed concrete, which is standard for Virginia bridge decks (4000 psi at 28 days, VDOT standard identification). The slabs were constructed to mimic the actual configuration of the slab, including the support beams. The actual deck and the lab specimen dimensions and reinforcing are presented in Figure 4.

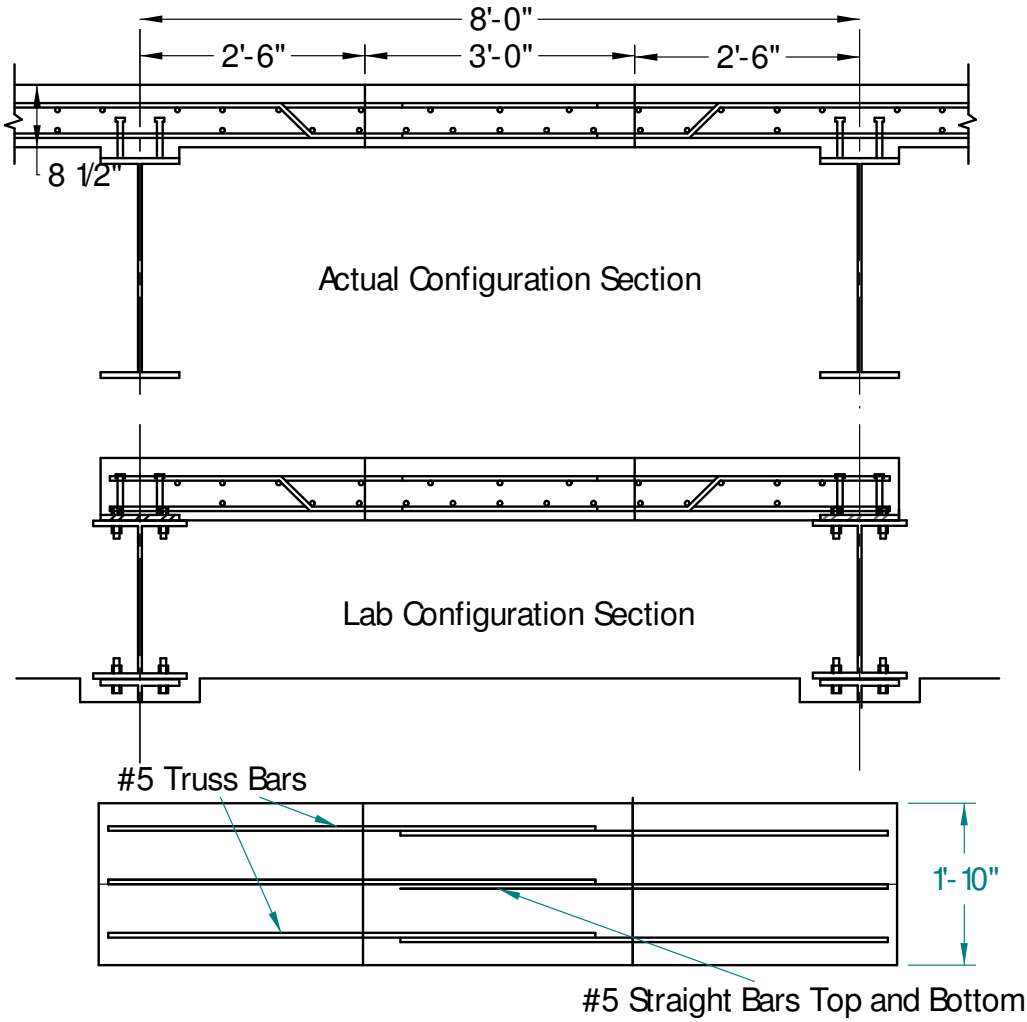

Figure 4. Lab Cast Slab Reinforcing Details

The actual bridge deck was constructed by closing one lane and shoulder of the bridge deck, and diverting traffic to the other lane. The closed lane and shoulder were then demolished and replaced. After construction of the first phase of the deck was completed, the new deck lane and shoulder were opened to traffic and the other lane and shoulder were closed, demolished and replaced. Finally, when both lanes and shoulders were completed the two sections were connected using a closure pour.

To generally replicate this sequence in the lab, both bridge decks (exterior sides) were cast at the same time, and allowed to cure for 30 days. Then, the closure pour was cast. The sequence is shown in Figures 5 and 6. The slab was connected by shear studs to the support beams, which were bolted to the reaction floor. This was done to provide restraint of shrinkage, similar to that provided by the actual bridge beams.

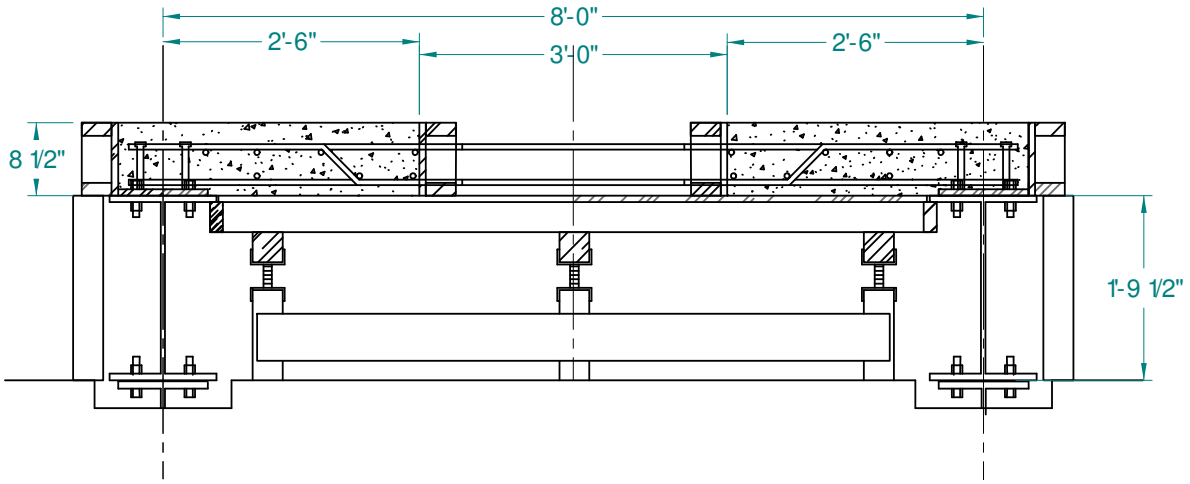

Figure 5. First Concrete Placement Setup

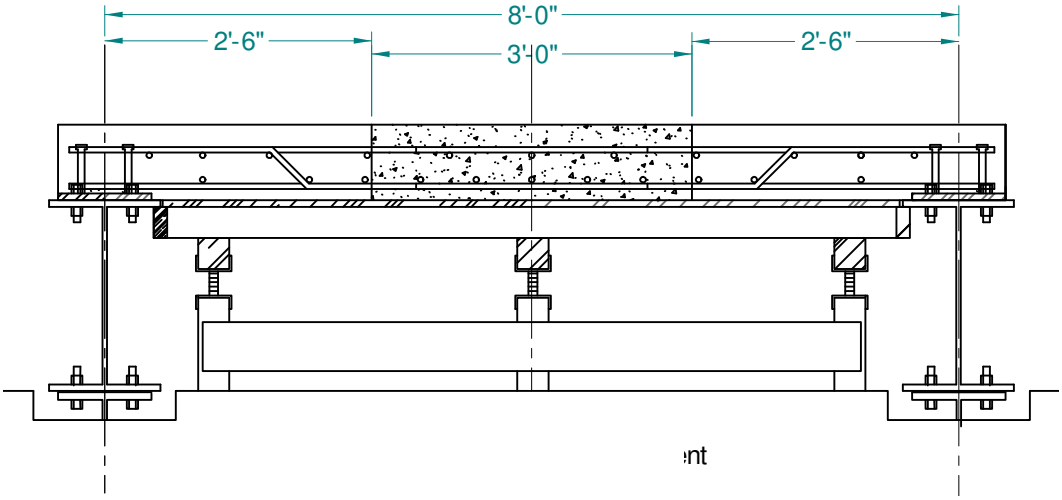

Figure 6. Second Concrete Placement Setup

Table 1 presents the mixture proportions for the two placements, total batched volume for the first and second placement were 4 cubic yards each.

Table 1. Cast Slab Mixture Proportions

Material	First Placement		Second Placement	
	Total Batched	Per Cubic Yard	Total Batched	Per Cubic Yard
Cement Type I, lb	2545	636	2535	634
Fly Ash, lb	635	159	665	166
Coarse Aggregate, lb	7060	1765	6980	1745
Fine Aggregate, lb	3840	960	3800	950
Water, lb	982	246	1130	283
Total, lb	15062	3766	15110	3778
AEA, fl. oz	6	1.5	5	1.25
MD W/R, fl. oz	76	19	76	19
Retarder, fl. oz	63	16	63	16

Concrete Material Property Testing

I-81 Slabs

Unit Weight, Percent Voids, and Percent Saturation Testing

Core samples were drilled from different locations from the bridge deck and closure pour concrete, as shown in Figures A.1 through A.4 in the Appendix. Core tests included unit weight, percent voids, and percent saturation of the concrete. Concrete properties were measured at the top and bottom for the deck and closure pour. Testing was conducted in accordance with ASTM C642-06, Standard Test Method for Density, Absorption, and Voids in Hardened Concrete.

Compressive Strength Testing

Seven core samples were drilled from the bridge deck and closure pour at locations shown in the Appendix, three from the deck and four from the closure pour. All coring was conducted using a water cooled diamond drill bit, with 4 in inside diameter. Strength tests were conducted accordance with ASTM C39 / C39M-10, Standard Test Method for Compressive Strength of Cylindrical Concrete Specimens.

Splitting Tensile Strength Testing

Seven core samples were drilled from the bridge deck and closure pour at locations shown in the Appendix, three from the deck, and four from the closure pour. They were tested in accordance with ASTM C496 / C496M-04, Standard Test Method for Splitting Tensile Strength of Cylindrical Concrete Specimens.

Modulus of Elasticity Testing

Core samples were drilled from the bridge deck and closure pour at locations shown in the Appendix, three from the deck, and four from the closure pour. Testing was conducted in accordance with ASTM C469 / C469M-10, Standard Test Method for Static Modulus of Elasticity and Poisson's Ratio of Concrete in Compression.

Lab Cast Slabs

Compressive Strength Testing

Four inch by eight inch compressive strength test cylinders were cast for both the first and second concrete placement. The cylinders were cured in the same manner and adjacent to the cast bridge deck sections. Compressive test were conducted at seven, 28, 56, and 90 days in accordance with ASTM C39 / C39M-10, Standard Test Method for Compressive Strength of Cylindrical Concrete Specimens. Two cylinders were tested at each age.

Splitting Tensile Strength Testing

Specimens were cast for the first and second placement using 4 in by 8 in plastic molds and were cured in the same manner and adjacent to the cast bridge deck sections. Tests were conducted at seven, 28, 56, and 90 days in accordance with ASTM C496 / C496M-04, Standard Test Method for Splitting Tensile Strength of Cylindrical Concrete Specimens. Two cylinders were tested at each age.

Modulus of Elasticity Testing

Likewise, specimens were cast for the first and second placement and cured in the same conditions and adjacent to the casted bridge deck sections. Testing was conducted at seven, 28, 56, and 90 days, in accordance with ASTM C469 / C469M-10, Standard Test Method for Static Modulus of Elasticity and Poisson's Ratio of Concrete in Compression. Two cylinders were tested at each age.

Corrosion-Related Tests and Observations

Visual Inspection

Visual inspection was conducted in two steps, using nondestructive and destructive methods. The nondestructive visual inspection included measurement of dimensions of the slabs and documentation of damage and cracking. Measurements were also made to determine the cold joints' widths using a feeler gauge. The destructive visual inspection required opening the specimens and visually observing the condition of the embedded ECR for corrosion and damage to the epoxy coating. Also noted were any deposits of calcium hydroxide, calcium carbonate and rust stains within the reinforcing bar trace. Finally, a scanning electron microscope (SEM) was used to examine several concrete specimens from the actual bridge slabs.

Cover Depth Measurements

The cover depth is the first line of defense against corrosive agents attacking the reinforcing steel, such as chloride and carbonation. Sufficient cover depth delays the attack of corrosion agents. To measure cover depths, reinforcing steel is detected by sending an electromagnetic field through the concrete. Steel interacts strongly with the electromagnetic field (Mehta and Monteiro, 2006).

Cover depths were measured in nine different locations in each 22 in by 54 in specimen, three on each side of the closure pour joints and three in the center of the closure pour using a Prometer 3, as illustrated in Figure 7. In addition cover depths were taken at the exposed side bars on each side of the specimens on the deck slab using both a ruler and Prometer 3 to confirm the concrete cover depth measurements.

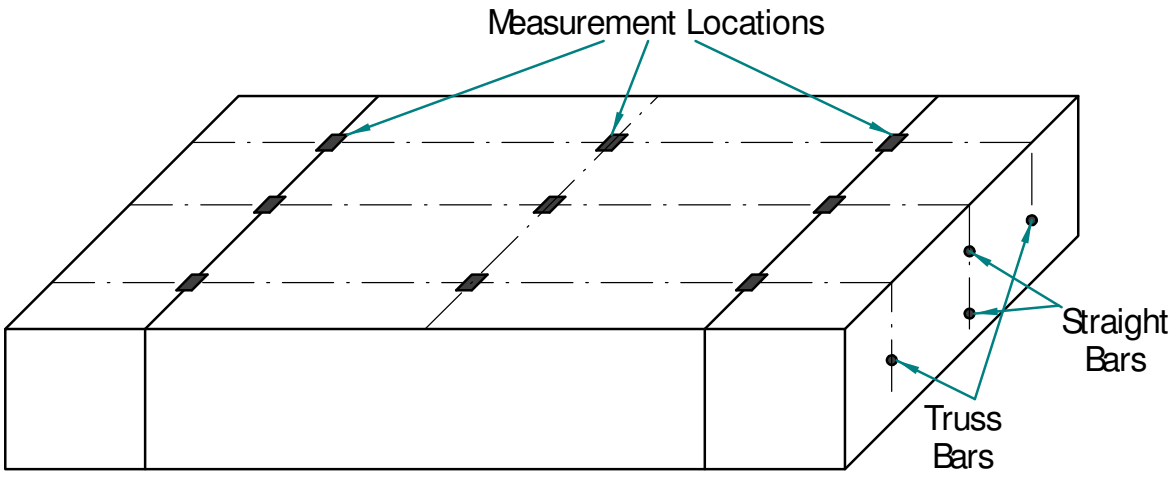

Figure 7. Cover Depth and Resistivity Measurement Locations

Concrete Resistivity

Measuring the concrete resistivity depends on the ions dissolved in the concrete pore liquid that carry the electrical current. This application can be used in different techniques such as a single point probe, two point probe, and a four point probe system. The most commonly used is the Werner Probe (four probe resistivity), which was developed for measuring soil resistivity. The readings do not indicate if the reinforcing steel is in active corrosion or not, but they give additional information on the potential for corrosion taking place in the structure and how resistive the concrete is to supporting corrosion (Polder et al., 2000).

Feliu et al. (1996) conducted tests using a disc method (single probe) using Newman's formula for onsite concrete resistivity measurements; the results are presented in Table 2.

Table 2. Single Probe Concrete Resistivity Interpretation

Concrete Resistivity (kΩ-cm)	Risk Levels
>100-200	Very low corrosion rates
10-100	Corrosion rate low to high
<10	Corrosion rate not controlled by resistivity

Source: Feliu et al. (1996).

In this research single point resistivity is used and it is represented by Equation 1

$$\rho = \frac{R\pi D^2}{4L} \qquad \text{(Eq. 1)}$$

where

ρ = resistivity of concrete (ohms-cm)
R = resistance of concrete (ohms)
D = diameter of the probe in contact with the concrete surface measuring resistance (cm)
L = clear cover depth + half the diameter of the reinforcing steel (cm)

Measurements were taken for each bar at the closure pour joint and at the center of the closure pour, as shown in Figure 7.

Half-Cell Potential

The test setup consists of a copper rod submerged in a saturated copper-copper sulfate solution and confined in a rigid tube with a porous plug at its bottom, which is now a copper/copper sulfate electrode (CSE) half-cell. An electrical junction device is mounted at the bottom of the CSE half-cell to provide continuity between the concrete surface and the porous plug. A sponge pre-wetted with an electrolyte is used to provide a low electrical resistance. The potential difference between the half-cell and the reinforcing steel is measured using a high impedance voltmeter. The detailed test setup is presented in Figure 8. Table 3 presents the data interpretation for the CSE half-cell potential for uncoated bar. Present published research does not provide guidelines for ECR. However, it has been shown that potentials in field structures built with ECR are normally distributed as they are for uncoated bar.

Half-cell potential readings were collected at the same locations where the cover depth readings were taken, as shown in Figure 7. Figure 9 shows where the exposed ends of the bars were drilled and tapped to create the circuit. Measurements were conducted in accordance with ASTM C876-91 using a CSE electrode. ASTM C876-91 states that the method is applicable for uncoated reinforcing steel, but it has been shown that it may be used on ECR (Brown et al., 2003).

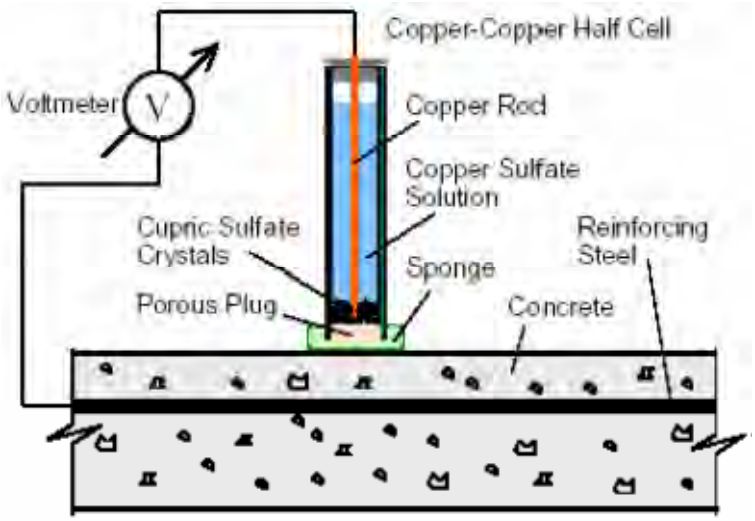

Figure 8. Half-Cell Potential Apparatus

Table 3. Corrosion Interpretation Using CSE Half-Cell

Measured Potentials (mV)	Corrosion Condition
> -200	Low (10% risk of corrosion)
-200 to -350	Intermediate corrosion risk
< -350	High (>90% risk of corrosion)

Source: ASTM C876-91.

Linear Polarization

This method gives real time readings of corrosion rate, but it cannot accurately calculate and predict total section loss or concrete spalling rate (Broomfield, 2007). It gives a snapshot of corrosion rate based on concrete temperature and moisture condition (Liu and Weyers, 2003). With current technology, corrosion rate provides the best measure of the rate of deterioration (Grantham et al., 1997; Broomfield, 2007).

The three-electrode polarization method (3LP method), shown in Figure 10, is one of the common methods used to measure corrosion rate. Three electrodes are required for the 3LP method: "working electrode" is the reinforcing steel embedded in the concrete, "counter electrode" is a metallic object used to apply the polarizing current, and "standard half-cell" is used to measure the response of the reinforcing steel to the current applied via the counter electrode (Clear, 1990). The test uses the Stern-Geary characterization of a polarization curve for corrosion. Corrosion current, $I_{corr,}$ is calculated using the Stern-Geary equation (Equation 2) (Clear, 1989; Liu and Weyers, 2003) and is connected to corrosion current density (i_{corr}) by dividing the corrosion current I_{corr} by an estimated reinforcing bar surface polarized area.

$$I_{corr} = \frac{\Delta I_{appl}(\beta_a \beta_c)}{1.2\Delta\phi(\beta_a + \beta_c)} = \frac{B}{R_p} \qquad \text{(Eq. 2)}$$

where

I_{corr} = corrosion current (mA)
I_{appl} = current required to polarize the rebar by different potential values from static potential
$\Delta\Phi$ = absolute value of cathodic polarization potential minus the natural electrical half-cell potential
β_a = anodic tafel slope (mV/decade) = 150 mV/decade
β_c = cathodic tafel slope (mV/decade) = 250 mV/decade
R_p = Polarization resistance (ohms)
B = constant value for steel in concrete between 26 and 52 mV, a values of 40 mV is used for the 3LP device.

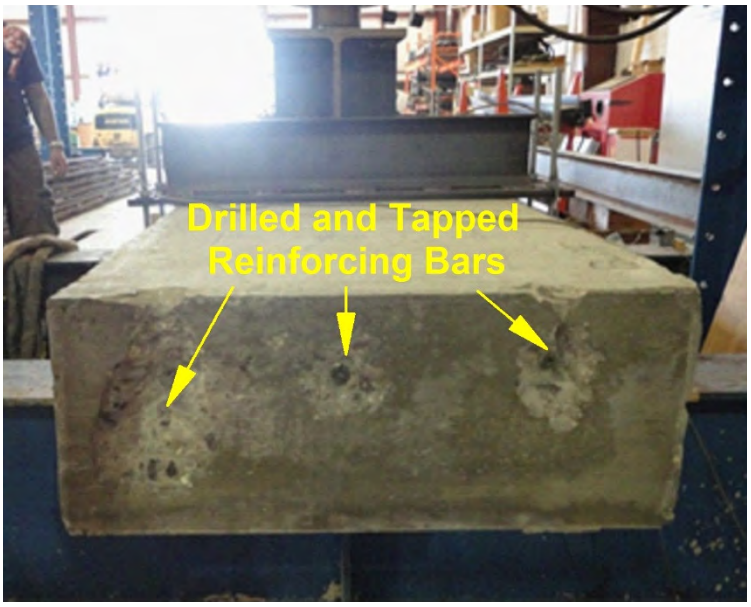

Figure 9. Drilled and Tapped Reinforcing Bars to Measure Corrosion Readings

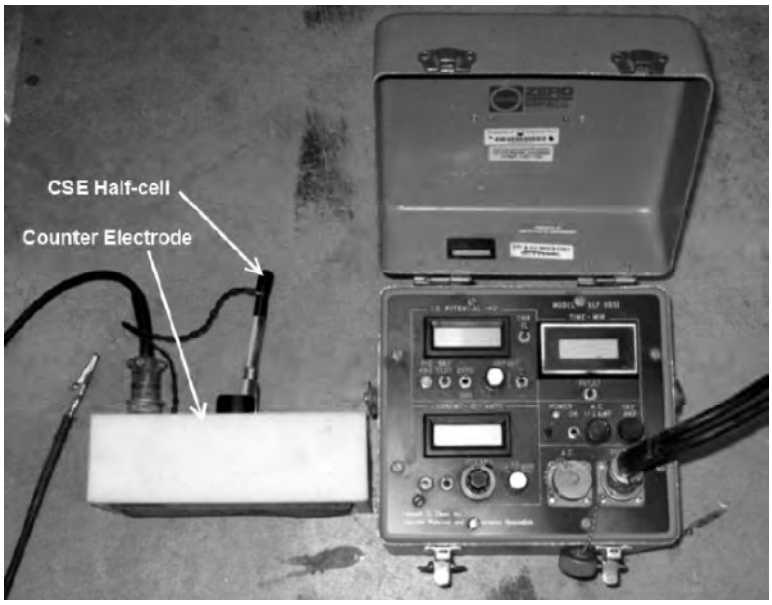

Figure 10. 3LP Device Setup. Photograph taken by Soundar S. G. Balakumaran (Balakumaran, 2010).

Interpretations of corrosion current density readings are provided by the 3LP developer for uncoated bar, but are generally considered in need of further evaluation (see Table 4). No interpretations are presented for ECR.

Table 4. Interpretations for Corrosion Current Density for 3LP Device

Corrosion Current Density, I_{corr} (mA/ft^2)	Corrosion Damage State
<0.2	No corrosion damage expected
0.2 – 1.0	Corrosion damage is possible in between 10 to 15 years
1.0 – 10	Corrosion damage expected between 2 to 10 years
>10	Corrosion damage expected in 2 years or less

Source: Clear, 1989.

The three-electrode polarization method (3LP method) was used to measure the corrosion current density (i_{corr}) of the ECR. The readings for the specimens were taken at the closure pour joint and at the middle of the closure pour for each bar from each side of each bar; see Figure 7.

Chloride Content

Two methods to measure chloride content in concrete are "acid soluble" (ASTM C1152/C 1152M) and "water soluble" (ASTM C1218/C1218 M). Both may be performed on powder samples after they are crushed smaller than the No.30 sieve. Table 5 presents one means of interpretation of acid soluble chloride values for uncoated bar.

Table 5. Chloride Contents Corrosion Risk

% Chloride by Mass of Cement	% Chloride by Mass of Sample (concrete)	Risk
<0.2	<0.03	Negligible
0.2 – 0.4	0.03 – 0.06	Low
0.4 – 1.0	0.06 – 0.14	Moderate
>1.0	>0.14	High

Source: Broomfeld, 2007.

Chloride samples were taken from 12 locations from the four deck slabs. The sample locations were adjacent to the cut slabs at the closure pour joints of Sides 1 and 2 as shown in the Appendix. Chloride content sample depth ranges were 2-3 and 3-4 in.

Concrete Shrinkage Testing

Concrete volume changes throughout its service life; it is dimensionally unstable (Mehta and Monteiro, 2006). This change is mainly caused by shrinkage and creep. Shrinkage is defined as a volumetric change without applying any sustained loads. Four types of concrete shrinkage are thermal, drying, autogenous, and carbonation (Aitcin et al., 1997; Holt and Leivo, 2004). Based on Holt and Leivo, shrinkage can be divided into two categories, early age and long term. Early shrinkage occurs in the first 24 hours and it consists of thermal and autogenous shrinkage, and is sensitive to internal stresses while concrete has a low strain capacity. Long term shrinkage occurs after 24 hours and consists of drying, thermal, carbonation, and further autogenous shrinkage (Holt and Leivo, 2004).

If concrete shrinkage is restrained, tensile stresses develop. In many cases, shrinkage restraint stresses are high enough to crack concrete. In the case of the closure pour joints, it is likely that the joints were open due to shrinkage restraint stresses. This study included the investigation of both unrestrained and restrained shrinkage.

There are many methods and models to calculate shrinkage and creep. Five shrinkage models were compared with the shrinkage readings on the lab cast slabs in the "Results" section. The five models are the American Concrete Institute (ACI 209R-92 model), Comite Euro-International Du Beton (CEB MC90 model), Gardner and Lockman (GL2000 model), Bazant-Baweja (B3 model), and AASHTO-LRFD.

Concrete shrinkage measurements were performed during both the first and second placement and are classified as restrained shrinkage and unrestrained shrinkage testing. The restrained shrinkage testing data collection was conducted for a period of 180 days on the surface of the lab cast slabs using DEMEC points. The unrestrained shrinkage was measured on concrete prisms

Slab Shrinkage Measurements

DEMEC points were placed using epoxy on the slab surface. A DEMEC gage was used to measure the length change between the points as shrinkage occurred as shown in Figure 11. Measurements were conducted for a period of 180 days for the deck on each side (first placement), the closure pour that connects each side of the deck (second placement), and across the closure pour joint (between the first and second placement). The time interval between the first and second placement was 30 days. Figure 12 illustrates the location of the DEMEC points.

Figure 11. A DEMEC Gage Measuring DEMEC Points

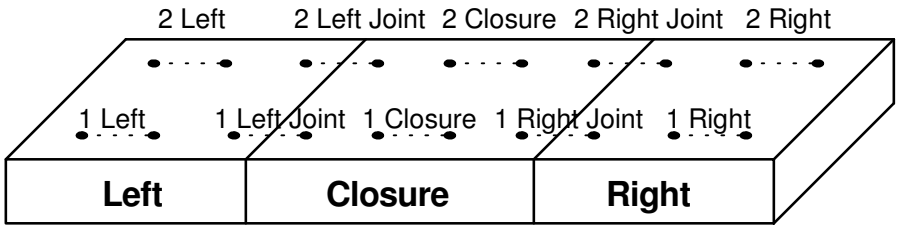

Figure 12. Location of DEMEC Points on Lab Cast Slab

Unrestrained Shrinkage Measurements

Unrestrained shrinkage measurements were conducted on concrete prisms with a dimension of 3 in x 3 in x 11in. Measurements were conducted in accordance with ASTM C157/C 157M-08, Standard Test Method for Length Change of Hardened Hydraulic-Cement Mortar and Concrete and performed for both the first and second placements. Three different curing conditions were evaluated:

1. The specimens were placed one day in mold, and then they were placed half an hour in lime bath before initial measurements were taken. After that, they were placed again six days in lime bath before placing them in the shrinkage room with a temperature of 73 ºF ± 3 ºF and 50% ± 4% relative humidity.

2. The specimens were placed one day in mold, and then they were placed half an hour in lime bath before initial measurements were taken. After that, they were placed again six days in lime bath before placing next to the laboratory slabs with an environment varying in temperature and humidity.

3. The specimens were placed six days in mold, after that initial measurements were taken before placing specimens next to the laboratory slabs with an environment varying in temperature and humidity.

Length change measurements were conducted for a period of 180 days. For the first placement, eight prisms were tested, three for the first curing condition, two for the second curing condition, and three for the third curing condition. For the second placement, ten prisms were tested, three each for the first and second curing conditions, and four for the third curing condition.

Water Ponding Testing

A ponding test was performed for each closure pour joint on each lab cast slab. Water was ponded for a period of 24 hours over each closure pour joint for each slab, as shown in Figure 13. The water ponding test was conducted to determine if the cast closure pour joints had opened wide enough to allow water leakage through the joint, similar to the deck joints.

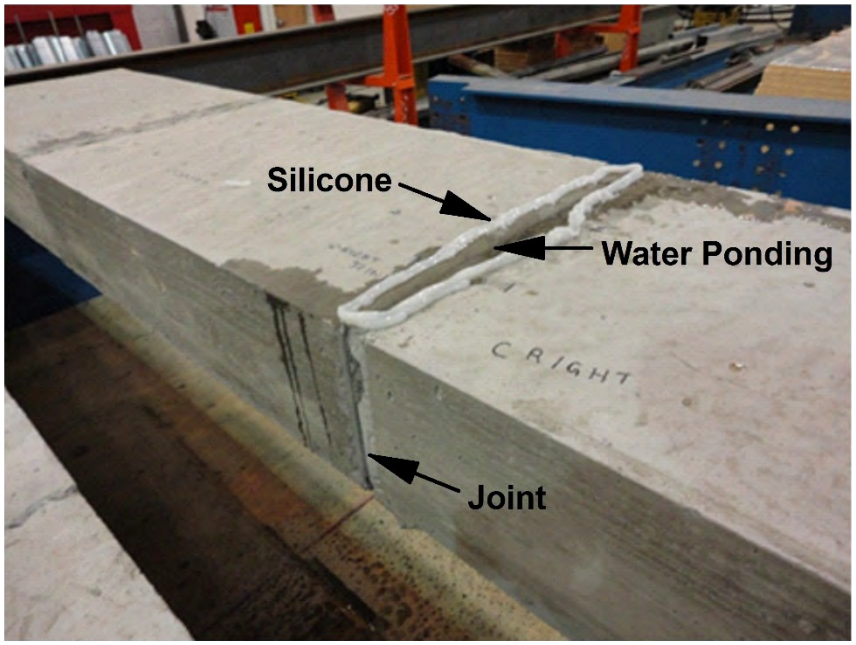

Figure 13. Water Ponding Test Across Joint

RESULTS AND DISCUSSION

Concrete Properties

Concrete Properties of I-81 Deck Slabs

Samples were cored from different locations from the slabs, eight from the closure and six from the deck concrete areas. Compressive strength, modulus of elasticity, unit weight, percent voids, and percent saturation were measured for those core samples. The results are presented in Tables 6 and 7 for the core samples from Virginia I-81 at Mile Marker 43 southbound travel lane (I81MM43SB) closure pour concrete and deck concrete.

Table 6. Closure Pour Compressive Strength, Modulus, and Unit Weight

Concrete Type	Core Number	Compressive Strength (psi)	Modulus of Elasticity (10^6 psi)	Unit Weight (lb/ft^3)
Closure	S1C1	6760	4.26	147.5
Closure	S1C2	8510	4.50	147.0
Closure	S2C1	7590	4.49	146.4
Closure	S2C4	7730	-	146.5
Average		7650	4.42	146.8

Table 7. Deck Compressive Strength, Modulus, and Unit Weight

Concrete Type	Core Number	Compressive Strength (psi)	Modulus of Elasticity (10^6 psi)	Unit Weight (lb/ft^3)
Deck	S2C2	4620	3.19	142.9
Deck	S2C3	6760	4.50	142.9
Deck	S2C5	5600	3.58	143.1
Average		5660	3.76	143.0

As shown in Tables 6 and 7, the closure concrete had a higher compressive strength, modulus of elasticity, and unit weight. Compressive strength is higher at lower w/c ratio and lower air content. Higher compressive strength results in an increased modulus of elasticity. The increase in unit weight indicates denser concrete, which indicates a lower air content.

As shown in Table 8, there is a slight difference in the concrete at the top and bottom of the closure pour concrete. On average the top section has a lower unit weight, compared to the bottom section, and a higher percentage of capillary voids. The average saturation percentage values are about equal for the top and bottom of the closure concrete.

From Table 9 it can also be observed that there is a difference in the concrete at the top and bottom of the deck. On average the top section has a lower unit weight, compared to the bottom section, which indicates differences in air content. The average saturation percentage values are lower for the top deck concrete than the bottom deck concrete. This can be related to a greater percentage of large capillary voids, as illustrated by the greater percent of total capillary voids in the top.

Table 8. Closure Pour Unit Weight, Percent Capillary Voids, and Percent Saturation

Concrete Type	Core Section	Unit Weight (lb/ft^3)	% Capillary Voids	% Saturation
Closure	S1C1 Top	146.6	12.7	85.5
	S1C1 Bottom	148.8	11.6	88.6
Closure	S1C2 Top	147.7	12.7	85.1
	S1C2 Bottom	148.6	11.5	84.5
Closure	S2C1 Top	147.9	12.4	85.4
	S2C1 Bottom	147.6	10.3	82.2
Closure	S2C4 Top	146.3	13.1	84.1
	S2C4 Bottom	147.4	11.7	84.1
Average Top		147.1	12.7	85.1
Average Bottom		148.1	11.3	84.8
Average Top and Bottom		147.6	12.0	85.0

Table 9. Deck Unit Weight, Percent Capillary Voids, and Percent Saturation

Concrete Type	Core Section	Unit Weight (lb/ft^3)	% Capillary Voids	% Saturation
Deck	S2C2 Top	146.4	12.6	82.5
	S2C2 Bottom	142.4	11.8	77.4
Deck	S2C3 Top	136.8	15.1	73.8
	S2C3 Bottom	146.4	10.5	77.2
Deck	S2C5 Top	140.1	12.7	71.6
	S2C5 Bottom	145.8	10.2	83.7
Average Top		141.1	13.5	76.0
Average Bottom		144.9	10.8	79.4
Average Top and Bottom		143.0	12.1	77.7

The differences between the closure and deck concrete are mainly due to the air content, moisture content, and pore size distribution. The closure concrete was denser compared to the deck concrete, which is shown in Tables 6 and 7. As presented in Tables 8 and 9, the closure and deck concrete results have the same pattern for the top and bottom sections with respect to density and percent capillary voids. This indicates that they are both affected by the same conditions.

Concrete Properties of Lab Cast Slabs

Fresh concrete properties of the first and second placement are shown in Table 10. The time between the first and second placement was 30 days. Tables 11 and 12 present the average of two specimens for the compressive strength, splitting tensile strength, and modulus of elasticity for the lab cast slabs.

Table 10. Fresh Concrete Properties of First and Second Placement

Property	First Placement	Second Placement
Unit Weight (lb/ft^3)	139.5	139.9
Slump (in)	4.75	5.5
Air Entrainment (%)	4	5.5
Temperature (ºF)	70	60

Table 11. First Placement Compressive Strength, Splitting Tensile, and Modulus of Elasticity

Age (Days)	Average Compressive Strength (psi)	Average Splitting Tensile Strength (psi)	Average Modulus of Elasticity (x 10^6 psi)
7	5930	610	4.05
14	5920	685	4.46
29	6510	720	4.53
56	6630	740	4.60
90	6650	760	4.58

Table 12. Second Placement Compressive Strength and Splitting Tensile Strength

Age (Days)	Average Compressive Strength (psi)	Average Splitting Tensile Strength (psi)
7	4930	585
28	6140	605
56	6280	645
90	6400	650

For the closure concretes, the compressive strength for the lab cast slabs at the age of 90 days was 19% less than the I-81 slab concrete at the age of 17 years. For the deck concrete, the compressive strength for the I-81 slabs at the age of 17 years was 17% greater than the lab cast slabs at the age of 90 days. Therefore, the lab cast specimens were considered to be reasonably similar to the actual deck specimens.

Corrosion Measurements

Corrosion measurements are discussed individually for I-81 deck slabs and lab cast slabs. These discussions include corrosion potential, resistivity, and corrosion current density measurements. All corrosion measurements are plotted as scatter diagrams, separately for the I-81 deck and lab cast slabs, in order to illustrate general observations between values. Also, the measurement differences between the joint and closure pour are presented.

Corrosion Measurements of I-81 Deck Slabs

The results for the corrosion related measurements for the I-81 deck slabs are presented in Tables 13 and 14 as the corrosion potentials, resistivity, and corrosion current density at the closure pour joint and within the closure pour. The locations of Slabs 1, 2, 4, and 7 are presented in the Appendix. Top bar cover depths ranged from 2.64 to 5.0 in for all of the slabs. VDOT specifies a cover depth for deck concrete of 2.5 in minus 0.0 in, plus 0.5 in. Thus, some of the ECR deck bars had a cover depth greater than the maximum of 3.0 in. Also, electrical continuity checks were performed between each ECR bar, which showed that all of the ECR was continuous between each bar combination.

As shown in Table 13, the Slab 1 potential measurements have a relatively high standard deviation, especially for Side 1. Slab 2, Slab 4, and Slab 7 are more uniform with a lower

standard deviation value than Slab 1. For the resistivity measurements, Slab 4 has a higher standard deviation value at Side 1 and 2 compared to the other slabs. The corrosion current density measurements for all the slabs are highly variable at Side 1 and 2 with standard deviation equal to or exceeding the average in some cases. Analyses of the results are presented later.

As shown in Table 14, the within closure pour potential measurements of Slab 7 and Slab 1, both have a relatively high standard deviation, especially for Side 1. Slab 2 and Slab 4 are more uniform with a lower standard deviation value than Slab 7 and Slab 1. For the resistivity measurements, Slab 7 and Slab 4 both have a higher standard deviation value at Side 1 and 2 compared to Slab 1 and Slab 2. The corrosion current density measurements for all the slabs are highly variable at Side 1 and 2 with standard deviation equal to or exceeding the average in some cases. Analyses of the results are presented later.

The higher resistivity readings in the closure concrete compared to the joint areas indicate a greater influence by the concrete plus the epoxy coating in these areas.

Table 13. Corrosion Measurements for I-81 Deck Slabs at Closure Pour Joints

		E_{corr} (mV)		R (kΩ-cm)		i_{corr} (mA/ft^2)	
Slab No.	**Bar No.**	**Side 1**	**Side 2**	**Side 1**	**Side 2**	**Side 1**	**Side 2**
Slab 1	TB	-413	-231	211	96	0.80	0.48
	BB 1	-261	-115	163	71	0.45	0.19
	BB 2	-199	-119	99	42	0.44	0.19
	BB 3	-277	-90	163	190	0.26	0.03
	Average	-288	-139	159	100	0.49	0.22
	STDV	90	63	46	64	0.23	0.19
Slab 2	TB	-148	-139	76	193	0.21	0.12
	BB 1	-119	-119	88	140	0.33	0.06
	BB 2	-166	-173	27	42	0.19	0.16
	BB 3	-147	-83	152	42	0.21	0.10
	Average	-145	-129	86	104	0.23	0.11
	STDV	19	38	51	75	0.06	0.04
Slab 4	TB	-58	-207	296	216	0.22	1.12
	BB 1	-71	-146	149	226	0.01	0.06
	BB 2	-66	-170	119	30	0.75	0.20
	BB3	-75	-129	126	259	0.03	0.08
	Average	-68	-163	172	183	0.25	0.36
	STDV	7	34	83	104	0.34	0.51
Slab 7	TB	-189	-135	72	55	0.03	1.36
	BB 1	-142	-180	62	66	0.07	0.03
	BB 2	-200	-164	139	83	0.84	0.68
	BB 3	-186	-172	153	168	0.41	0.33
	Average	-179	-163	106	93	0.34	0.60
	STDV	26	20	46	51	0.37	0.57

Corrosion Measurements of I-81 Deck Slabs – Closure Pour vs. Closure Joints

Corrosion measurements for the I-81 deck slabs are plotted as a scatter diagram comparing the closure pour corrosion measurements versus the closure joint measurements, as shown in Figures 14 through 16.

Figure 14 shows a scatter diagram for corrosion potentials versus resistivity for I-81 deck slabs. As shown, the corrosion potentials for the closure pour and the closure joints measurements are less than -200 mv indicating low corrosion activity, although some values show higher corrosion activity. As previously stated, resistivity measurements for the closure pour indicate higher resistivity compared to the closure joint measurements. Higher resistivity indicates better concrete quality or an interference from the epoxy coating since it is generally considered a nonconductive material if not saturated.

Table 14. Corrosion Measurements for I-81 Deck Slabs Within Closure Pour

		E_{corr} (mV)		R (kΩ-cm)		i_{corr} (mA/ft^2)	
Slab No.	**Bar No.**	**Side 1**	**Side 2**	**Side 1**	**Side 2**	**Side 1**	**Side 2**
Slab 1	TB	-422	-287	233	350	0.45	0.15
	BB 1	-296	-188	233	396	0.18	0.06
	BB 2	-207	-190	233	233	0.21	0.06
	BB 3	-323	-226	233	233	0.10	0.01
	Average	-312	-223	233	303	0.24	0.07
	STDV	89	46	0	83	0.15	0.06
Slab 2	TB	-136	-135	96	194	0.05	0.02
	BB 1	-130	-128	161	82	0.20	0.02
	BB 2	-149	-175	91	194	0.05	0.04
	BB 3	-167	-135	180	198	0.07	0.03
	Average	-146	-143	132	167	0.09	0.03
	STDV	16	21	45	57	0.07	0.01
Slab 4	TB	-171	-210	256	119	0.07	0.44
	BB 1	-127	-173	145	131	0.01	0.02
	BB 2	-201	-174	217	19	0.22	0.08
	BB 3	-199	-151	107	443	0.01	0.02
	Average	-175	-177	181	178	0.08	0.14
	STDV	35	24	68	184	0.10	0.20
Slab 7	TB	-5.8	-151	93	226	0.01	0.39
	BB 1	-202	-213	177	56	0.03	0.03
	BB 2	-221	-224	723	326	0.38	0.57
	BB 3	-12.3	-171	98	110	0.16	0.13
	Average	-110	-190	273	180	0.15	0.28
	STDV	117	34	302	121	0.17	0.24

Figure 15 shows a scatter diagram for corrosion potentials versus corrosion current density for I-81 deck slabs. As shown, corrosion current density measurements for the closure joints indicate higher corrosion activity compared to the closure pour measurements. Most of the measurements of the closure pour are less than 0.2mA/ft^2. The closure joint measurements are highly variable showing low to higher corrosion rates. However, in general the corrosion rates increase with higher negative values of the corrosion potentials for both the closure and joint values, but more so for the joint measurements.

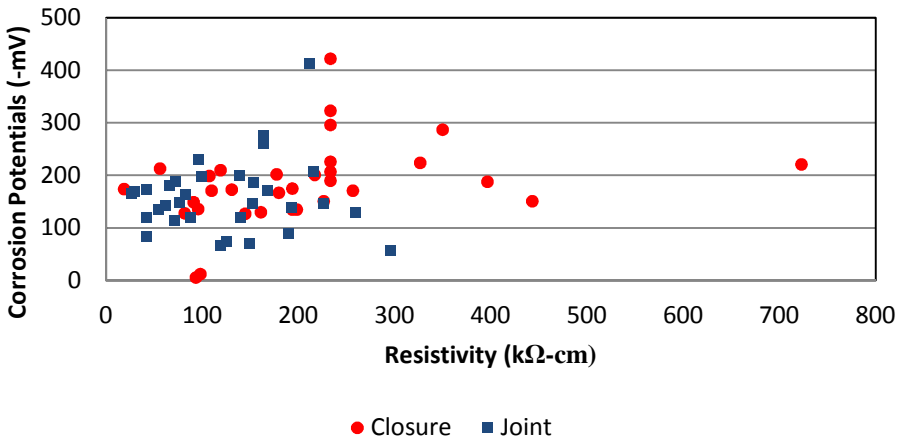

Figure 14. Corrosion Potentials vs. Resistivity for I-81 Slabs

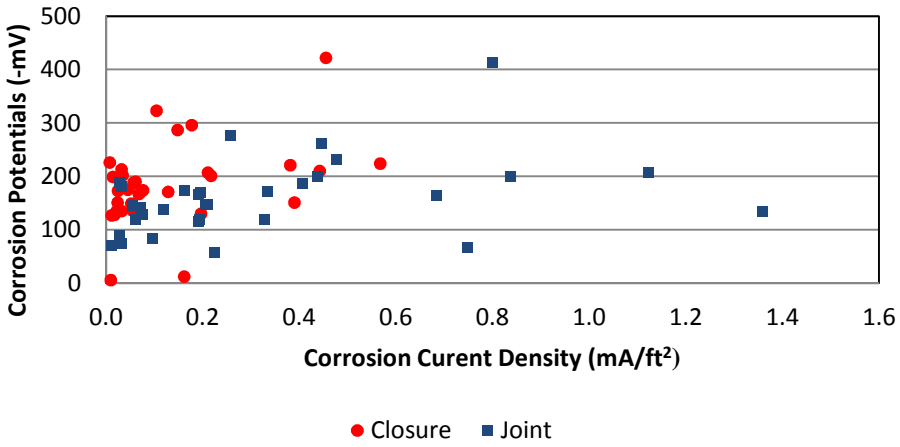

Figure 15. Corrosion Potentials vs. Corrosion Current Density for I-81 Slabs

Figure 16 shows a scatter diagram for resistivity versus corrosion current density for I-81 deck slabs. It can be noticed that the resistivity measurements for the closure pour indicate higher resistivity compared to the closure joint measurements. Higher resistivity indicates more of an influence by the concrete and/or an interference from the epoxy coating since it maybe more of a nonconductive material. Corrosion current density measurements for the closure joints indicate higher corrosion activity compared to the closure pour measurements. Most of the measurements of the closure pour are less than 0.2mA/ft^2, which indicates very low corrosion activity. While the closure joint measurements are highly variable showing low to high corrosion activity.

Thus, from the scatter diagrams, there is higher corrosion activity across the closure joints based on the corrosion current density measurements.

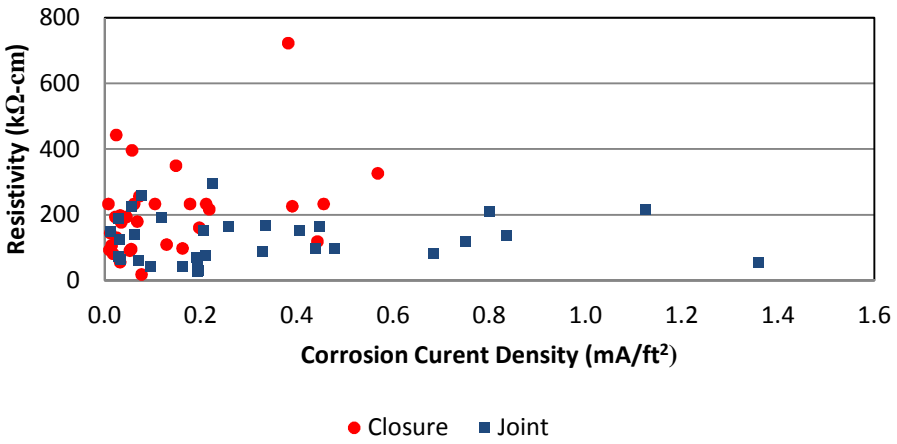

Figure 16. Resistivity vs. Corrosion Current Density for I-81 Slabs

Corrosion Measurements of Lab Cast Slabs

Tables 15 and 16 present the results of the corrosion related measurements for the lab cast decks. Cover depths were measured with a range from 2.64 to 4.2 in for the three slabs. These results are similar to the deck slabs cover depths range. The tests were conducted on three bars (TB, BB 1, and BB 3) out of four bars on each side of the slabs. Since the top bar is located directly over the bottom middle rebar, this made the cover meter ineffective in locating the bottom bar. Electrical continuity checks were performed for each single bar between Side 1 and 2, and it showed that each spliced ECR bar is continuous between both sides, as shown in Figure 17.

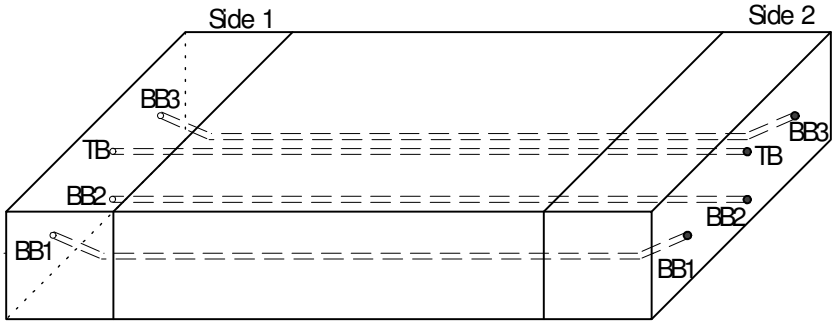

Figure 17. Continuity Reading Locations for Lab Cast Slab

Table 15. Corrosion Measurements for Lab Cast Slabs at Closure Pour Joints

Slab No.	Bar No.	E_{corr} (mV)		R (kΩ-cm)		i_{corr} (mA/ft^2)	
		Side 1	Side 2	Side 1	Side 2	Side 1	Side 2
Slab A	TB	-25	-123	169	138	0.010	0.023
	BB 1	-65	-150	67	140	0.011	0.007
	BB3	-40	-190	113	164	0.004	0.004
	Average	-43	-154	116	147	0.01	0.01
	STDV	20	34	51	15	0.00	0.01
Slab B	TB	-70	-124	22	125	0.015	0.009
	BB 1	-103	-157	61	134	0.011	0.105
	BB 3	-91	*	239	*	0.136	*
	Average	-88	-141	107	129	0.05	0.06
	STDV	17	23	116	7	0.07	0.07
Slab C	TB	-139	-142	108	47	0.015	0.005
	BB 1	-188	-104	72	72	0.005	0.007
	BB 3	-144	-149	157	132	0.127	0.007
	Average	-157	-132	112	83	0.05	0.01
	STDV	27	24	43	44	0.07	0.00

Note: * Data unavailable, ECR could not be located.

Table 16. Corrosion Measurements for Lab Cast Slabs Within Closure Pour Concrete

Slab No.	Bar No.	E_{corr} (mV)		R (kΩ-cm)		i_{corr} (mA/ft^2)	
		Side 1	Side 2	Side 1	Side 2	Side 1	Side 2
Slab A	TB	-40	-129	233	161	0.003	0.017
	BB 1	-76	-155	217	110	0.006	0.003
	BB 3	-42	-190	205	256	0.003	0.003
	Average	-53	-158	218	176	0.00	0.01
	STDV	20	31	14	75	0.00	0.01
Slab B	TB	-65	-133	126	89	0.022	0.012
	BB 1	-107	-210	135	62	0.007	0.005
	BB 3	-47	*	166	*	0.006	*
	Average	-73	-172	142	75	0.01	0.01
	STDV	31	54	21	19	0.01	0.01
Slab C	TB	-150	-138	326	215	0.010	0.009
	BB 1	-206	-106	443	133	0.004	0.005
	BB 3	-145	-143	256	280	0.019	0.004
	Average	-167	-129	342	209	0.01	0.01
	STDV	34	20	94	74	0.01	0.00

Note: * Data unavailable.

As shown in Table 15, the potential, resistivity, and corrosion current density measurements at the closure pour joints indicated a relatively uniform condition with a low standard deviation for all three lab cast slabs. Analyses of the results are presented later. Some results for Slab B bottom bar (BB 3) are not presented since the ECR could not be located as stated previously.

As shown in Table 16, the potential, resistivity, and corrosion current density measurements within the closure pour concrete indicate relatively uniform conditions with a low standard deviation for all three lab cast slabs. Analyses of the results are presented later. Some results for Slab B bottom bar (BB 3) are not presented since the ECR could not be located as previously stated.

Corrosion Measurements of Closure Pour – I-81 Slabs vs. Lab Cast Slabs

Corrosion measurements for the closure pour are plotted as a scatter diagram comparing the I-81 slabs measurements versus the lab cast slabs measurements, as shown in Figures 18 through 20.

Figure 18 shows a scatter diagram for corrosion potentials versus resistivity for the closure pour of the I-81 slabs versus the lab cast slabs measurements. As observed, the corrosion potentials for the I-81 deck slabs indicate higher corrosion activity compared to the lab cast slab measurements. The lab cast slabs' corrosion potentials are less than -200 mv, which indicates low corrosion activity, while the I-81 deck slabs measurements are indicating higher corrosion activity with corrosion potentials greater than -200 mv. The resistivity measurements for the I-81 deck and lab cast slabs indicate high resistivity with a similar range of measurements.

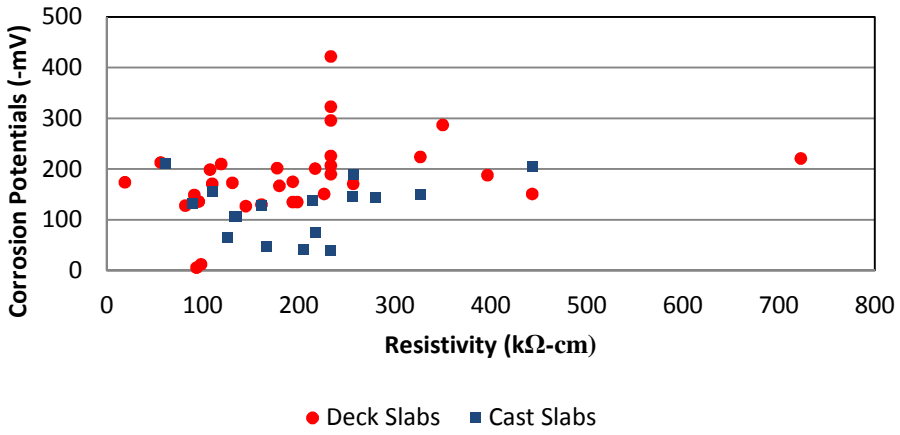

Figure 18. Closure Pour Corrosion Potentials vs. Resistivity for Deck vs. Cast Slabs

Figure 19 shows a scatter diagram for corrosion potentials versus corrosion current density for the closure pour of the I-81 slabs versus the lab cast slabs' measurements. As shown, the corrosion potentials for the I-81 deck slabs indicate higher corrosion activity compared to the lab cast slabs measurements. Corrosion current density measurements for the I-81 deck slabs indicate higher corrosion activity compared to the lab cast slabs' measurements, with the deck slab corrosion current density generally increasing with corrosion potentials. All of the measurements of the lab cast slabs are less than 0.2mA/ft^2, which indicates no corrosion activity.

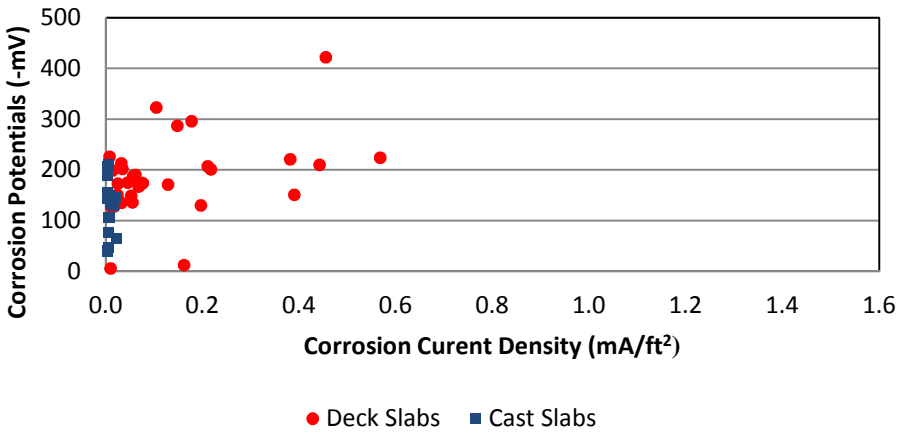

Figure 19. Closure Pour Corrosion Potentials vs. Corrosion Current Density for Deck vs. Cast Slabs

Figure 20 shows a scatter diagram for resistivity versus corrosion current density for the closure pour of the I-81 slabs versus the lab cast slabs measurements. The resistivity measurements for the I-81 deck and lab cast slabs have a similar range of measurements.

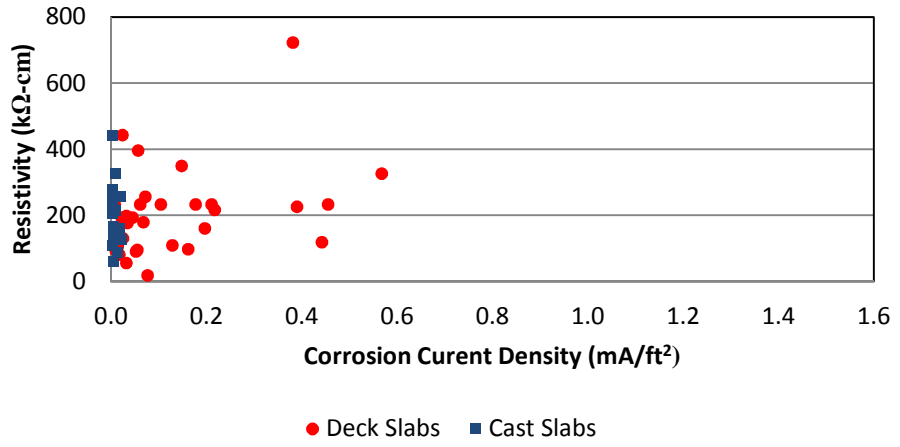

Figure 20. Closure Pour Resistivity vs. Corrosion Current Density for Deck vs. Cast Slabs

It can be noticed from the scatter diagrams of the closure pour that there is higher corrosion activity at the I-81 deck slabs compared to the lab cast slabs based on the corrosion current density measurements. The lab cast slabs indicated no corrosion activity based on the corrosion current density measurements, which were less than 0.2 mA/ft^2.

Corrosion Measurements of Closure Pour Joints – I-81 Slabs vs. Lab Cast Slabs

Corrosion measurements for the closure pour joints are plotted as a scatter diagram comparing the I-81 slabs measurements versus the lab cast slabs measurements, as shown in Figures 21 through 23.

Figure 21 shows a scatter diagram for corrosion potentials versus resistivity for the closure pour joints of the I-81 slabs versus the lab cast slabs measurements. As shown, the

corrosion potentials for the I-81 deck slabs indicate somewhat of a higher corrosion activity compared to the lab cast slabs' measurements. The lab cast slabs' corrosion potentials are less than -200 mv, which indicates low corrosion activity, while the I-81 deck slabs measurements are indicating higher corrosion activity with corrosion potentials greater than -200 mv. The resistivity measurements for the I-81 deck and lab cast slabs have a similar range of measurements.

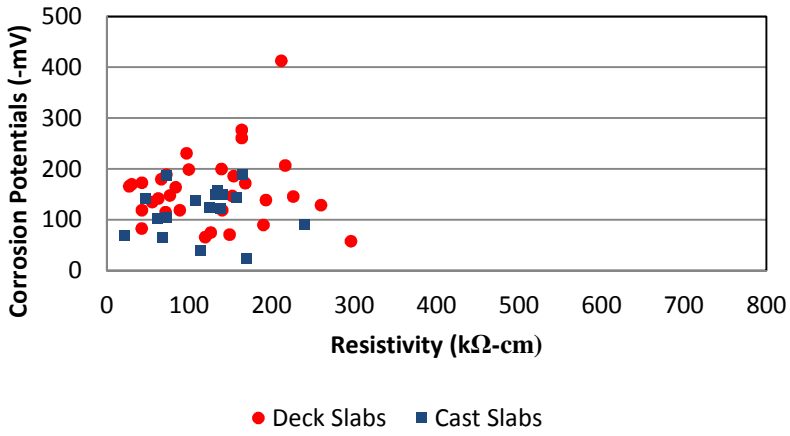

Figure 21. Closure Joints Corrosion Potentials vs. Resistivity for Deck vs. Cast Slabs

Figure 22 shows a scatter diagram for corrosion potential versus corrosion current density for the closure pour joints of the I-81 slabs versus the lab cast slabs measurements. Corrosion current density measurements for the I-81 deck slabs indicate higher corrosion activity compared to the lab cast slabs measurements. All of the measurements of the lab cast slabs are less than 0.2 mA/ft^2.

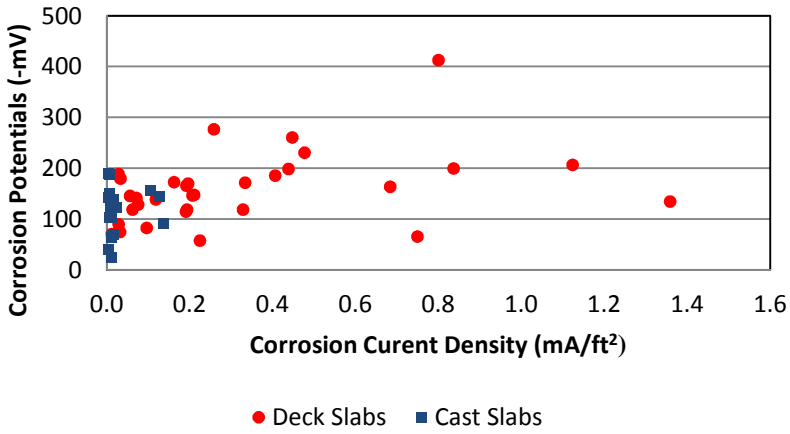

Figure 22. Closure Joints Corrosion Potentials vs. Corrosion Current Density for Deck vs. Cast Slabs

It can be noticed from the scatter diagrams of the closure pour joints that there is higher corrosion activity at the I-81 deck slabs compared to the lab cast slabs based on the corrosion current density measurements. The lab cast slabs indicated no corrosion activity based on the corrosion current density measurements, which were less than 0.2 mA/ft^2.

Chloride Measurements in I-81 Deck Slabs

The results for the chloride content in I-81 closure pour joints are presented in Table 17. Powdered samples were taken from 12 locations on the four deck slabs. The samples' locations were adjacent to the cut slabs at the closure pour joints of sides 1 and 2 as shown in the Appendix. Chloride content depth ranges were at 2-3 and 3-4 in. Acid soluble chloride contents were determined in accordance with ASTM C1152.

The results indicate that chlorides are present at general bars depths (3-4 in) in the closure pour joints varying from 1.64 to 4.69 lb/yd^3. Also, the chloride contents at average depths of 2.5 and 3.5 in are similar rather than decreasing with depth. This indicates that the leaking closure pour joints facilitated the chloride movement to the bar depth. The chloride values are sufficient to initiate corrosion of the ECR as determined by Brown with a range of 0.13 to 3.00 lb/yd^3 for ECR (Brown, 2002).

Table 17. Chloride Content in Closure Pour Joints of I-81 Deck Slabs

Sample Location	Joint	Sample Range (in)	Chloride Content (lb/yd^3)
Adjacent to Test Section One	Side 1	2-3	4.21
		3-4	4.40
	Side 2	2-3	4.11
		3-4	3.83
Adjacent to Test Section Two	Side 1	2-3	3.26
		3-4	3.50
	Side 2	2-3	3.20
		3-4	4.69
Adjacent to Test Section Three	Side 1	2-3	0.08
		3-4	2.47
	Side 2	2-3	1.80
		3-4	2.30
Adjacent to Test Section Four	Side 1	2-3	2.84
		3-4	2.72
	Side 2	2-3	2.62
		3-4	2.65
Adjacent to Test Section Seven	Side 1	2-3	4.65
		3-4	3.44
	Side 2	2-3	1.35
		3-4	1.64
Adjacent to Test Section Eight	Side 1	2-3	3.68
		3-4	3.55
	Side 2	2-3	2.19
		3-4	1.99
Average	Side 1	2-3	3.12
		3-4	3.35
	Side 2	2-3	2.55
		3-4	2.85
STDV	Side 1	2-3	1.48
		3-4	0.63
	Side 2	2-3	0.91
		3-4	1.07

The results for the chloride content in the I-81 closure pour are presented in Table 18. Powdered samples were taken from six locations from the two deck slabs. The samples locations were at the center of the closure pour as shown in the Appendix. Chloride content sample ranges were at 0-1, 1-2, 2-3, and 3-3.5 in. Acid soluble chloride contents were determined in accordance with ASTM C1152.

Table 18. Chloride Content in Closure Pour of I-81 Deck Slabs

Sample Location	Sample Range (in)	Chloride Content (lb/yd^3)
Slab One (1-2)	0-1	15.3
	1-2	3.0
	2-3	0.3
	3-3.5	-
Slab One (1-4)	2-3	12.2
	3-4	-
	2-3	0.2
	3-3.5	0.3
Slab One (1-6)	0-1	14.1
	1-2	2.7
	2-3	0.3
	3-3.5	-
Slab Two (2-2)	0-1	16.0
	1-2	7.9
	2-3	1.0
	3-3.5	-
Slab Two (2-4)	0-1	11.4
	1-2	2.4
	2-3	0.6
	3-3.5	-
Slab Two (2-6)	0-1	14.3
	1-2	3.0
	2-3	-
	3-3.5	0.7
Average	0-1	13.88
	1-2	3.80
	2-3	0.48
	3-3.5	0.50
STDV	0-1	1.77
	1-2	2.31
	2-3	0.33
	3-3.5	0.28

The results indicate that chlorides are generally present in low concentrations, which are considered as background readings of less than 0.5 lb/yd^3, at general bars depths (2-3.5 in) with the exception of one value of 1.0 lb/yd^3.

The closure pour joints' chloride contents are higher, varying from 1.64 to 4.69 lb/yd^3, than the closure pour chloride contents, which vary from 0.2 to 1.0 lb/yd^3 at the general bar depths. Also, the chloride contents for the closure pour joints are similar at average depths of 2.5 and 3.5 in, while the closure pour chloride contents decrease with depth. Thus confirming that leaking closure pour joints facilitated the chloride movement to the bar depth, while for the

closure pour the concrete cover depth was acting as a barrier against chlorides reaching the bar depth.

Chloride Permeability in I-81 Deck Slabs

The results for the chloride permeability in I-81 closure pour joints are presented in Table 19. One 4 in diameter core was taken from each of slabs 1 and 2. To maintain the moisture content, the core samples were sealed with shrink wrap, aluminum foil and duct tape. Then the cores were sliced 2 in from the top (top sample) and another 2 in (bottom sample). Chloride permeability sample ranges were at 0-2 in (top sample) and 2-4 in (bottom sample) for both. Testing was first conducted for the slices, top and bottom, in the as received moisture content and saturated condition. After testing in the as-received moisture condition, the top and bottom slices were tested again, in accordance to AASHTO T277, by vacuum saturating the slices. This test measures the concrete resistance with the unit in coulombs.

Table 19. Chloride Permeability in Closure Pour of I-81 Deck Slabs, Coulombs

	As-Received Moisture		Saturated	
Core	Top (0-2 in)	Bottom (2-4 in)	Top (0-2 in)	Bottom (2-4 in)
1-1	880	826	2371	1722
1-2	446	969	1362	1882
2-1	547	784	1639	1919
2-2	543	700	1375	1610
Average	604	820	1687	1783

The results indicate that chloride permeability is very low for the as received moisture condition specimens since all of the measurements were below 1000 coulombs. For the saturated specimens, with one exception, the values ranged between 1000 and 2000 coulombs, which indicates low chloride permeability. Core 1-1 was the only value that was over 2000 coulombs; this indicates that the chloride permeability is moderate. The results demonstrate the lower potential for chloride ingress for in-field moisture conditions versus saturated conditions.

Visual Observations

Photographs of Visual Inspection

Samples were cut from different places on the bridge deck across the joints as shown in the Appendix. The samples were stored without damaging and exposing the ECR embedded into the concrete by keeping the concrete around the ECR in place.

Figures 23 and 24 present the visual inspection of samples C2-S1 Bottom Bar 1 and C2-S1 Top Bar 2, as shown in the Appendix. As shown in Figure 23, arrow 1, the bar is corroded across the joint as indicated by the change of epoxy color. Figure 24 shows signs of spotted deposits, arrow 2, on the bar surface, with less signs of corrosion, arrow 3, as compared to the top bar shown in Figure 23. Figure 25 shows white and yellow deposits in the concrete along the bar trace underneath the bar, at the location shown by arrow 2 in Figure 24.

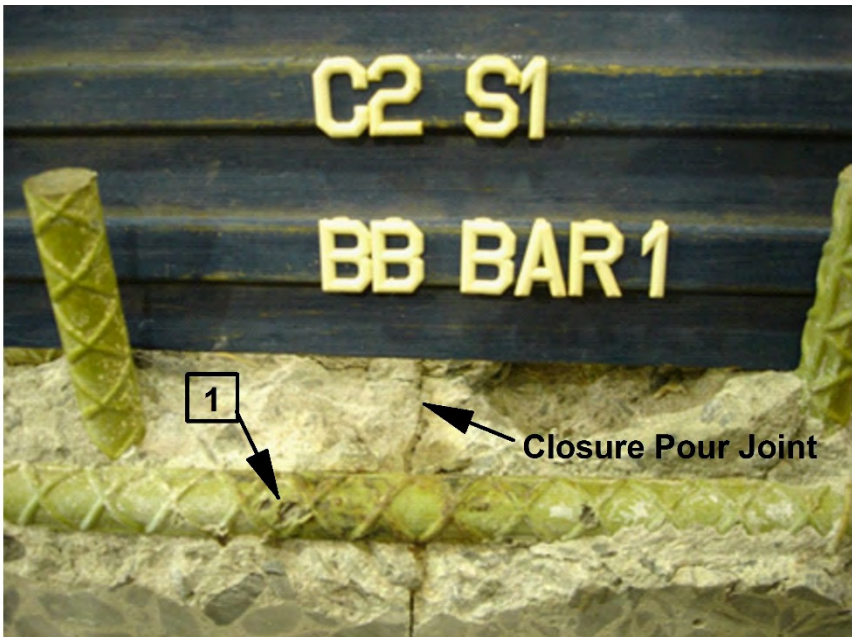

Figure 23. C2-S1 Bottom Bar 1

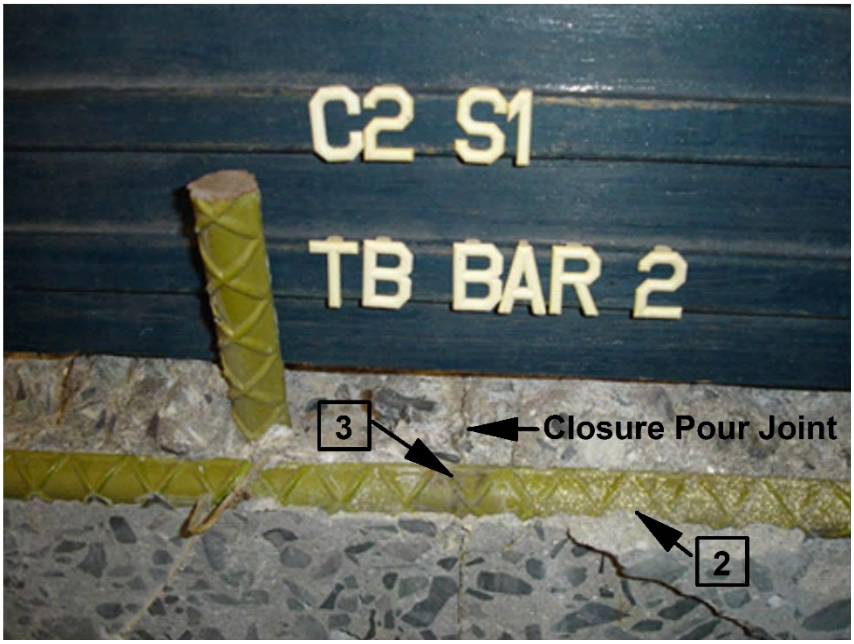

Figure 24. C2-S1 Top Bar 2

Figure 25. C2-S1 Top Bar 2 After Removing Bar

The sample shown in Figure 26 was taken from the bottom of slab three across joint one, as shown in the Appendix. Figure 26 shows some precipitation, arrow 4, at the top of the bar and corrosion, arrow 5, at the bottom of the bar. Samples shown in Figures 27 and 28 were taken from the top of the same slab. Figure 27 shows some white and yellow deposits on the bar at arrow 6, and Figure 28 shows the yellow precipitation in the bar trace at the location of arrow 7.

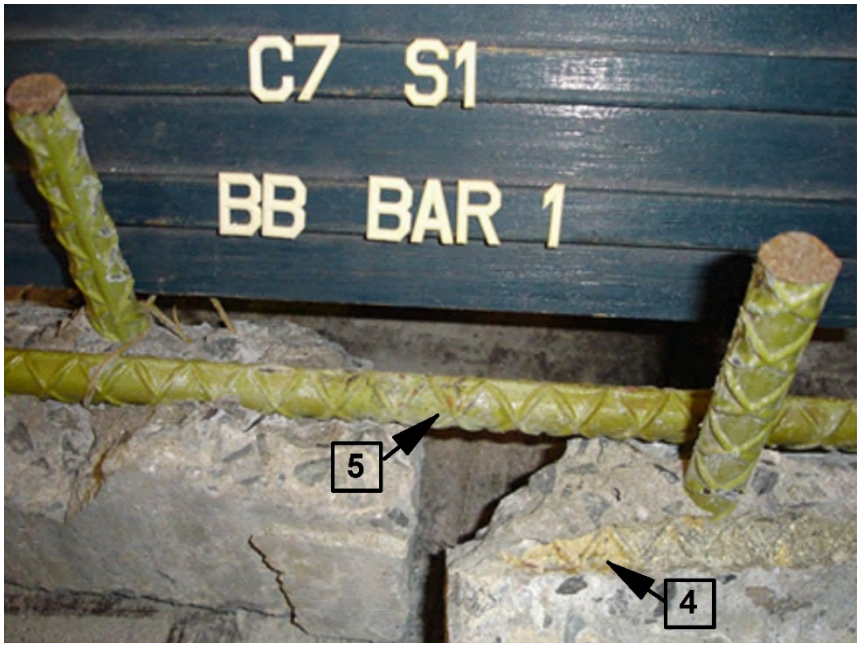

Figure 26. C7-S1 Bottom Bar 1

Figure 27. C7-S1 Top Bar 2 Without Concrete

Figure 28. C7-S1 Top Bar 2 After Removing Bar

The samples shown in Figures 29 and 30 were taken from the top of slab four across joint two, as shown in the Appendix. Samples shown in Figures 31 and 32 were taken from the bottom of the same slab. Figures 29 and 30 show some deposits, arrow 9, at the top of the bar and corrosion, arrow 8, at the bottom of the bar. Figures 31 and 32 show the bar at the top of the bottom bar with some precipitation, arrow 11, and corrosion, arrow 10, at the joint.

Figure 29. C8-S2 Top Bar 2 Without Concrete

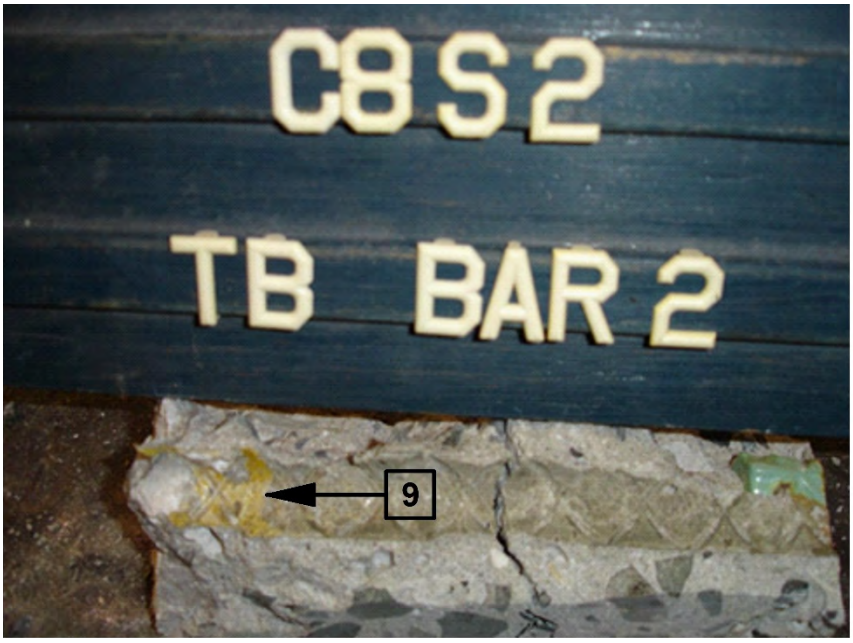

Figure 30. C8-S2 Top Bar 2 After Removing Bar

Figure 31. C8-S2 Bottom Bar 1 Without Concrete

Figure 32. C8-S2 Bottom Bar 1 After Removing Bar

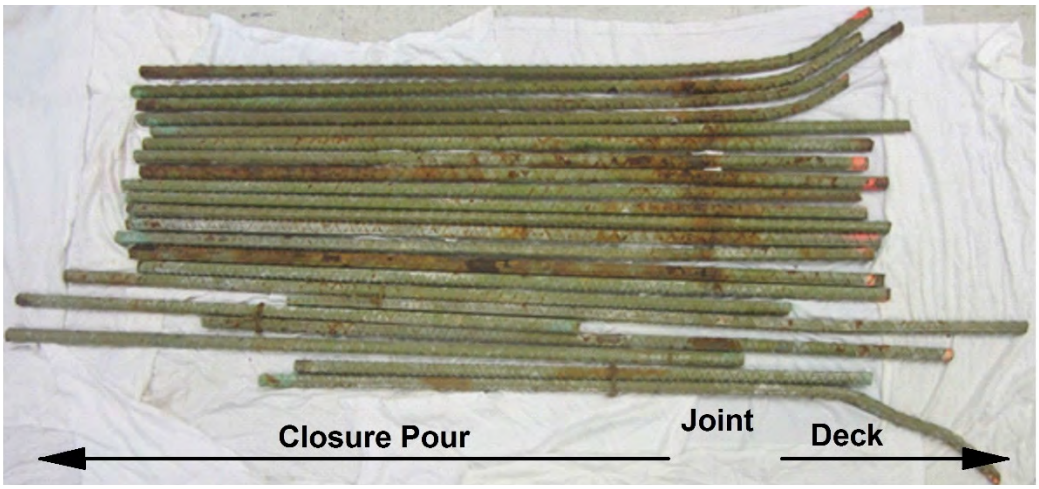

Figure 33. Corrosion Extent of Extracted ECR Bars

For all of the samples taken from different locations from the slabs, deposits and corrosion were observed at the joint and moving along the bar and bar trace in both the closure and the deck concrete. Although corrosion was noticed in some bars, the epoxy coating was difficult to peel off the reinforcing bar. The bars were soaked for two weeks in water to aid the epoxy debondment from the bars to have a closer look at the corrosion under the coating. This had no effect on debonding the epoxy from the bars, although there were some places were the coating was peeled off due to the corrosion on the bar, as shown in Figure 31.

The extent of the corrosion of the ECR beyond the joint interface is illustrated in Figure 33, a photograph of the ECR bars recovered at the job site. As shown, corrosion of the ECR varied from 4 in to 31 in along the bar on each side of the joint.

Scanning Electron Microscopy of Concrete Sample at Joint

After opening the samples across the joints and observing yellow and white precipitation in the ECR trace, further analysis was required to identify the chemistry of the precipitations. Six concrete images and corresponding chemical compositions were taken using an SEM.

Figure 34 presents a typical SEM micrograph of sample. The two image areas shown in Figure 34 are I81MM43SB-1 on a yellow deposit area and I81MM43SB-2 outside the yellow deposit. Table 20 presents the chemical composition of the two locations. Location 1 shows high carbon content compared to location 2, which indicates that the yellow precipitation is calcium carbonate where water penetrates the closure pour, dissolves the $Ca(OH)_2$ in the hydrated cement, then reacts with carbon dioxide in the air to form calcium carbonate. The presence of calcium carbonate within the ECR trace away from the joint indicates a higher level of water content within the interface between the ECR and concrete. Water movement within the ECR trace would have been from the joint line inward, indicating a higher void volume at ECR- Concrete interface. Location 2 shows high silicon content compared to location 1, which indicates that it is hydrated cement since silicates are commonly present in hydrated cement as tricalcium silicate (C_3S) and dicalcium silicate (C_2S).

The higher percent of voids at the ECR-concrete interface would allow water, chloride, and oxygen to penetrate along the ECR-concrete interface some distance and corrode the ECR as shown in Figure 33.

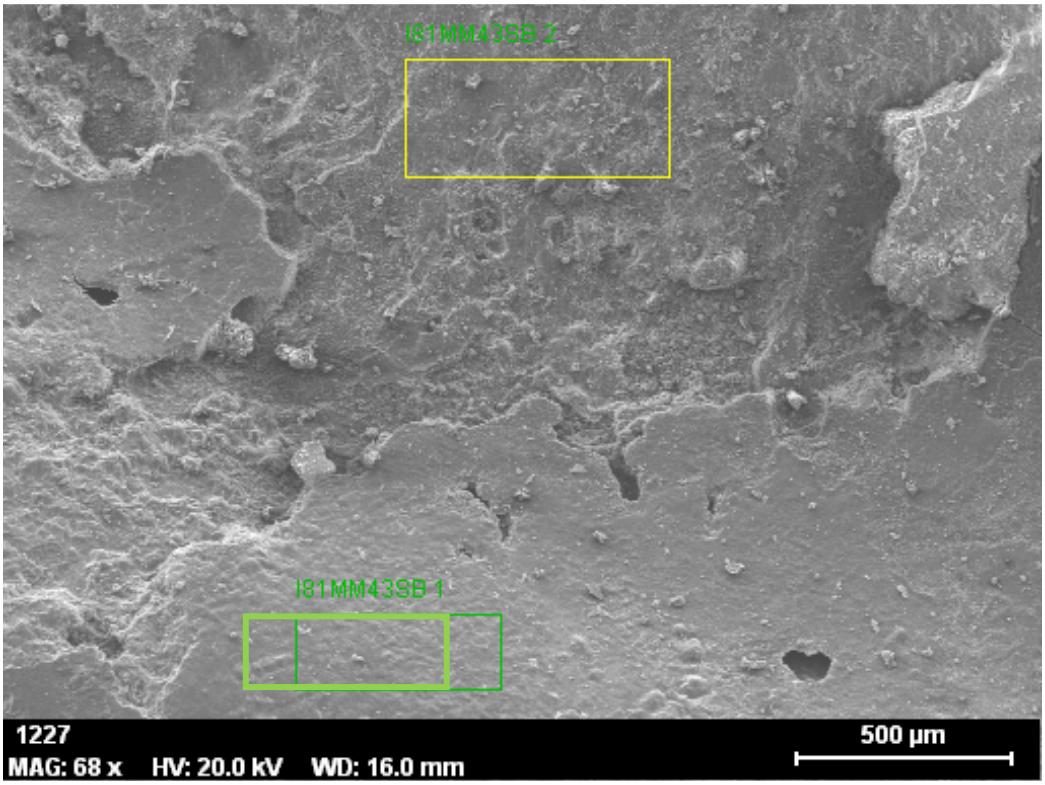

Figure 34. Sample One SEM Micrograph I81MM43SB-1 and I81MM43SB-2

Table 20. Sample One EDS Chemical Composition I81MM43SB-1 and I81MM43SB-2

	Mass Percent (%)									
Spectrum	**C**	**O**	**Na**	**Mg**	**Al**	**Si**	**K**	**Ca**	**Ti**	**Fe**
I-81MM43SB-1	16.57	58.19	1.76	0.92	1.18	2.71	0.49	17.21	0.43	0.55
I-81MM43SB-2	5.21	57.32	0.81	1.04	2.22	10.30	1.22	19.55	0.14	2.19
Difference Between 1 and 2	11.36	0.87	0.95	-0.12	-1.04	-7.59	-0.73	-2.34	0.29	-1.64

Joint Opening Measurements

Closure joint openings from the I-81 bridge deck were measured using a feeler gauge to determine the approximate construction joint width. Some parts of the closure joints, at Side 1 and 2, were filled with debris on the four I-81 bridge deck slabs, which made it difficult to measure the true joint width in certain locations. The measurements were taken on the side of the slabs from top to bottom, since the top surface of the slabs were rough and there was more filling of the joints. There was a possibility for denting or damaging the tip of the feeler gauge, which may have affected its precision.

For slab one, the construction joint width for Side 1 and 2 ranged from 0.009 to 0.016 in. Slab two joint measurements ranged from 0.010 to 0.016 in. Slab three joint measurements ranged from 0.009 to 0.020 in. Slab four joint measurements ranged from 0.010 to 0.025 in.

This indicates that the closure joints are not fully sealed and are strongly influenced by the shrinkage of the concrete, which causes these joints to open. For reinforced concrete under service load ACI 224R recommends that the crack width be kept below 0.007 in for deicing chemicals (chlorides) (ACI Committee 224, 2001). This threshold value has been exceeded in the I-81 bridge deck closure joints, which increases the risk of chloride attack, as demonstrated by previous results. Also of note, these measurements were taken after removal, so the restraint had been released. The in-situ crack widths were not measured but were most likely somewhat wider.

Shrinkage Bars and Deck Shrinkage

Unrestrained Shrinkage

Figures 35 and 36 present unrestrained drying shrinkage for the first and second concrete placement for the lab cast slabs. A total of eight prism specimens were tested for the first placement, and a total of ten prism specimens were tested for the second placement. Each set of prism specimens, for the first and second placement, were separated into three different curing conditions, presented in Table 21. For the first placement eight prisms were tested, three for the first curing condition, two for the second curing condition, and three for the third curing condition. For the second placement ten prisms were tested, three each for the first and second curing conditions, and four for the third curing condition.

Table 21. Prism Specimens Curing Conditions

Series	Curing Conditions Description
1	Place one day in mold, and then place half an hour in lime bath before taking initial measurements. After that place specimens again six days in lime bath before placing them in shrinkage room.
2	Place one day in mold, and then place half an hour in lime bath before initial measurements were taken. After that place specimens again six days in lime bath before placing next to the slabs in ambient conditions.
3	Place six days in mold, after the initial measurements before placing specimens next to the slabs in ambient conditions.

The shrinkage behavior of the first placement was similar for Series 1, 2, and 3, as shown in Figure 35. They exhibited a similar trend throughout the 180 days of testing duration, and the final readings at 180 days were 700 microstrain. Each series presented in Figure 35 is the average of all prisms per series. Series 1, which was placed in the shrinkage room, exhibited a slower shrinkage rate than Series 2 and 3, which were placed in ambient conditions next to the lab cast slabs. The temperature in the shrinkage room was set to 72^{o} F ± 3^{o} F.

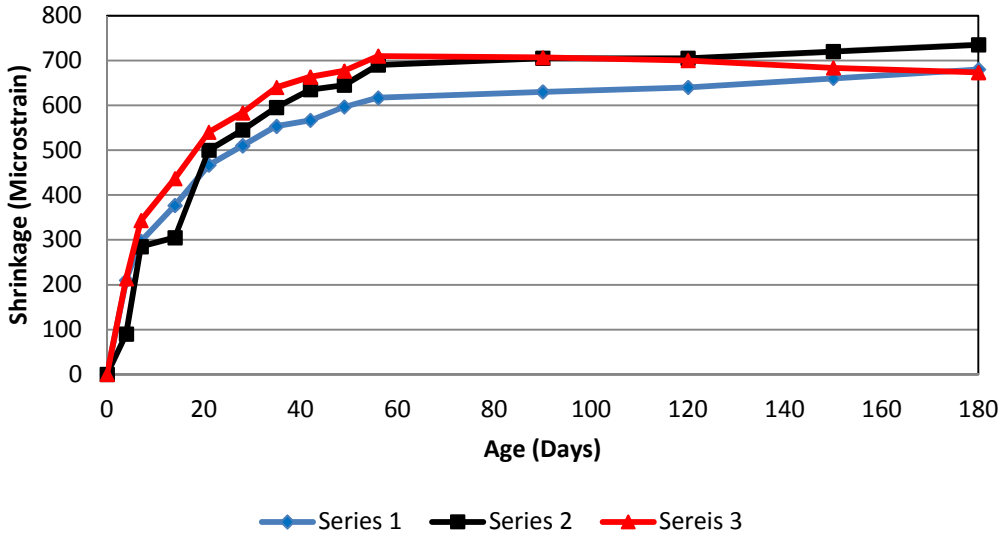

Figure 35. Average Drying Shrinkage for All Series of First Placement

The shrinkage behavior of the second placement was also similar for Series 1, 2, and 3, as shown in Figure 36. Each series presented in Figure 36 is the average of all prisms per series. They exhibited a similar trend throughout the 180 days of testing duration. The final readings at 180 days were 740 microstrain, 5% more than the first placement. Series 1, which was placed in the shrinkage room, exhibited a slower shrinkage rate, while Series 2 and 3 were placed in ambient conditions next to the lab cast slabs and they had a similar shrinkage rate.

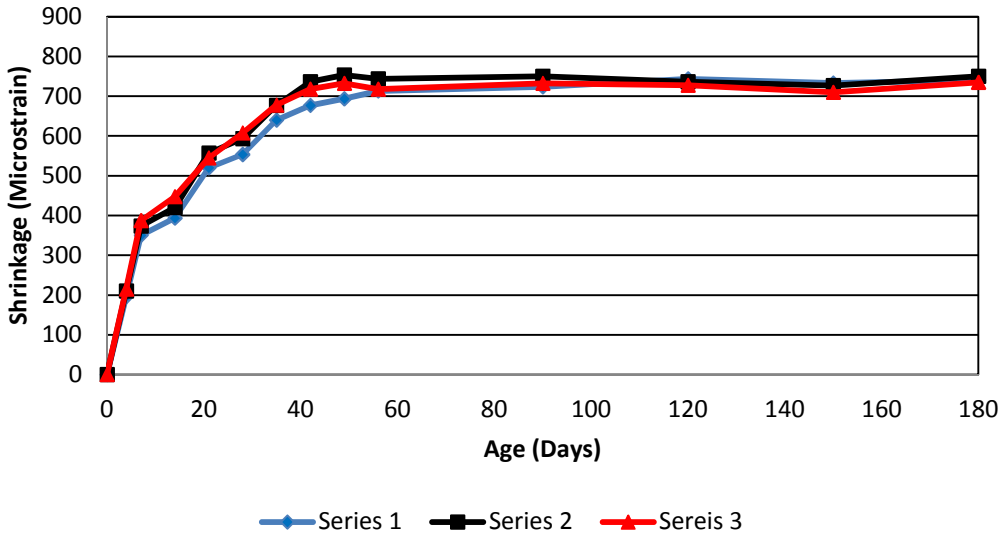

Figure 36. Average Drying Shrinkage for All Series of Second Placement

Restrained Shrinkage

Figures 37 through 39 present restrained drying shrinkage for the first and second concrete placements for the three lab cast slabs and across the two joints. A DEMEC gage was used to measure the length change between the points as shrinkage occurred. Four shrinkage

readings were taken seven days after the first concrete placement, two readings from the right deck and two from the left deck. After 30 days the closure pour placement was made. Two shrinkage readings were measured on the closure, and an additional four measurements were measured across the joint, seven days after the second placement (see Figure 12). Shrinkage readings were measured at regular intervals for 180 days. The three slabs were labeled as Slab A, Slab B, and Slab C.

Figure 37 presents the shrinkage of the left and right sides of the three slabs for the first placement of concrete. Each series is the average of two pairs of DEMEC points. All of the shrinkage readings follow the same trend with final readings between 275 and 330 microstrain at 180 days. The second placement (closure pour) was placed 30 days after the first placement, and it is represented with a dashed line in Figure 37. At the time the closure pour was placed, approximately 50% of the shrinkage had occurred. The rate of shrinkage slows after the placement of the closure pour. This is due to both a naturally slowing rate of shrinkage with age, and the restraint of shrinkage strain by the support beams, once the closure is in place.

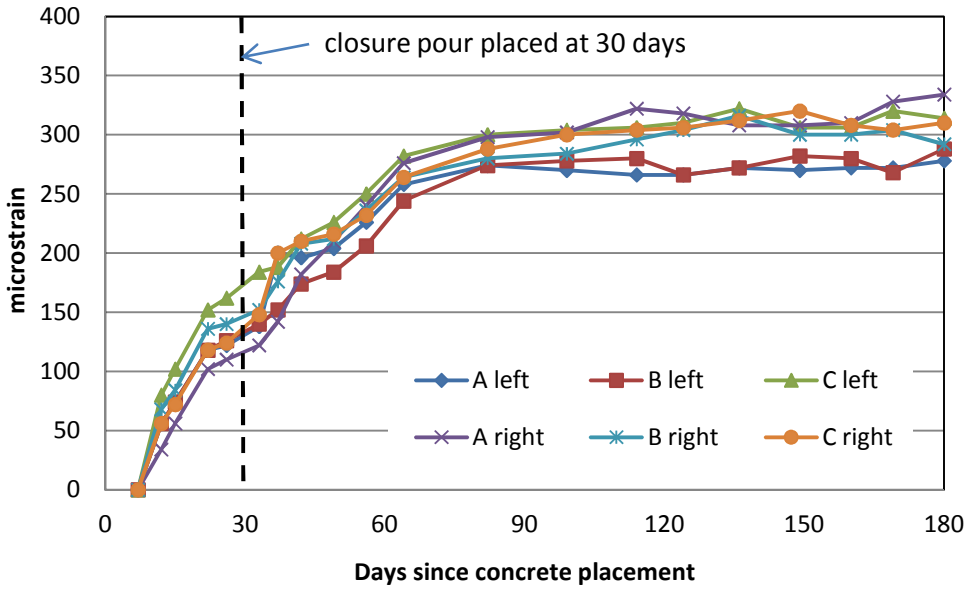

Figure 37. Slab Shrinkage Readings for First Placement

Figure 38 presents the shrinkage of the closure concrete for the three slabs. Each curve is the average of two pairs of DEMEC points. The shrinkage for the closure concrete was slightly higher than the first placement, with shrinkage at 180 days between 410 and 440 microstrain.

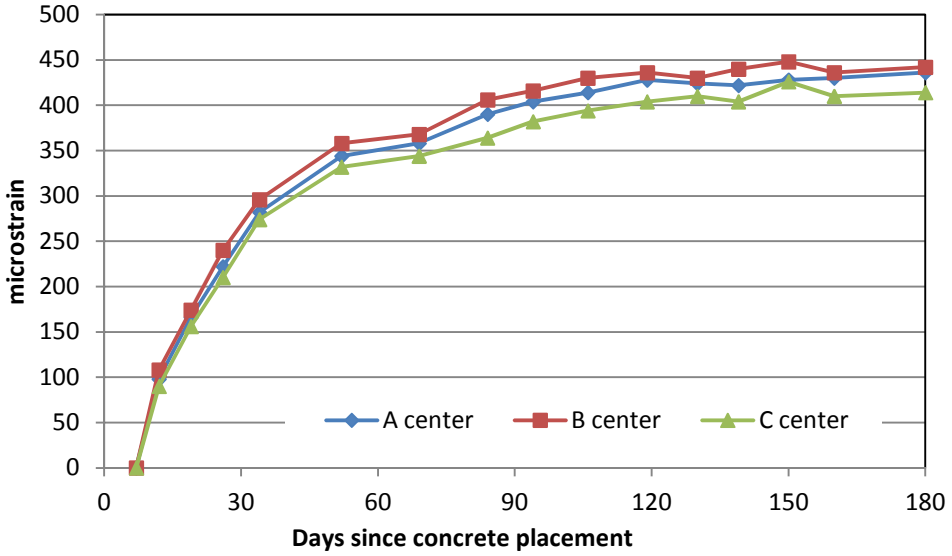

Figure 38. Slab Shrinkage Readings for Second Placement

Figure 39 presents the shrinkage measured across the joints of the three slabs. There is considerably more scatter in these readings, most likely due to the opening of the joint. The shrinkage at 180 days varies from 75 to 300 microstrain. This is much less than the shrinkage measured for the monolithic concrete, which is also most likely due to the opening of the joints.

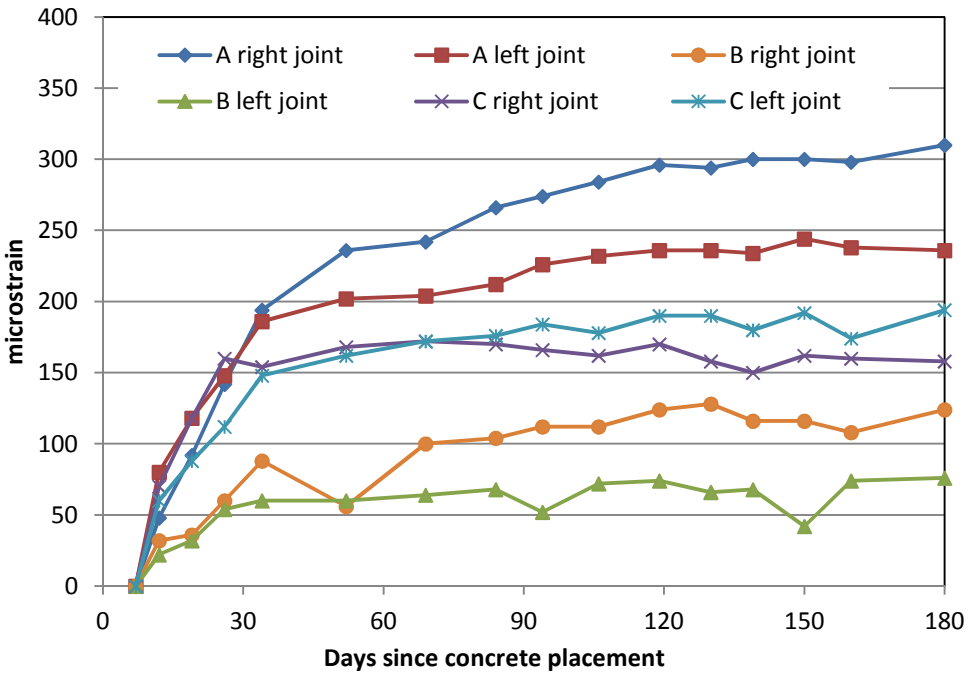

Figure 39. Shrinkage Readings for Joints Between Deck and Closure

The unrestrained shrinkage had a higher rate of shrinkage compared to restrained shrinkage. The majority of the unrestrained shrinkage occurred prior to 50 days, for the first and

second placement, for the three tested series. For the restrained shrinkage it took over 80 days for the majority of the shrinkage to occur. The magnitude of the unrestrained shrinkage was much higher than the restrained shrinkage, ~700 με compared to ~350 με. This is due to both the restraint of shrinkage by the support beams and reinforcing, and the greater volume-to-surface area ratio of the slabs.

DEMEC Readings After Unbolting Lab Cast Slabs

Table 22 presents the change in strain of the lab cast slabs upon release of the restraining effect of the support beams. The DEMEC points on the slabs were measured before unbolting them from the support beams, and after. After unbolting the slabs, the DEMEC gauge readings were fluctuating, so the slabs were left for 24 hours to relax, after which the measured readings stabilized.

A negative reading indicates contraction, which would be expected upon release of the restraint. Slab A and C generally exhibited the expected behavior of a restrained end condition, although the displacements were very small. Slab B exhibited unexpected behavior compared to the other slabs. This might be due to some debris inside the joint affecting the results.

Table 22. Change in Strain Before and After Unbolting

Location	Point	Slab A Difference (με)	Slab B Difference (με)	Slab C Difference (με)
Left	1	24	12	60
	2	0	X	-24
Left Joint	1	-52	80	-500
	2	-52	-156	-428
Center	1	72	-68	60
	2	-16	20	80
Right Joint	1	-180	X	-424
	2	-280	144	-560
Right	1	0	X	-24
	2	148	240	68

X indicates a problem with the DEMEC points, so a reading could not be made.

Comparison of Unrestrained Shrinkage Models

Five models were used to predict the unrestrained shrinkage and compare it with the actual measured results. The average relative humidity in the laboratory varied, from 40% to 92%, throughout the testing period, from December 2010 to June 2011. Figure 40 presents a comparison for the five models for 50% RH. The two models with the best predictions are the ACI 209 model and the GL2000 model. Both models, however, predict a slower rate of shrinkage development than was measured.

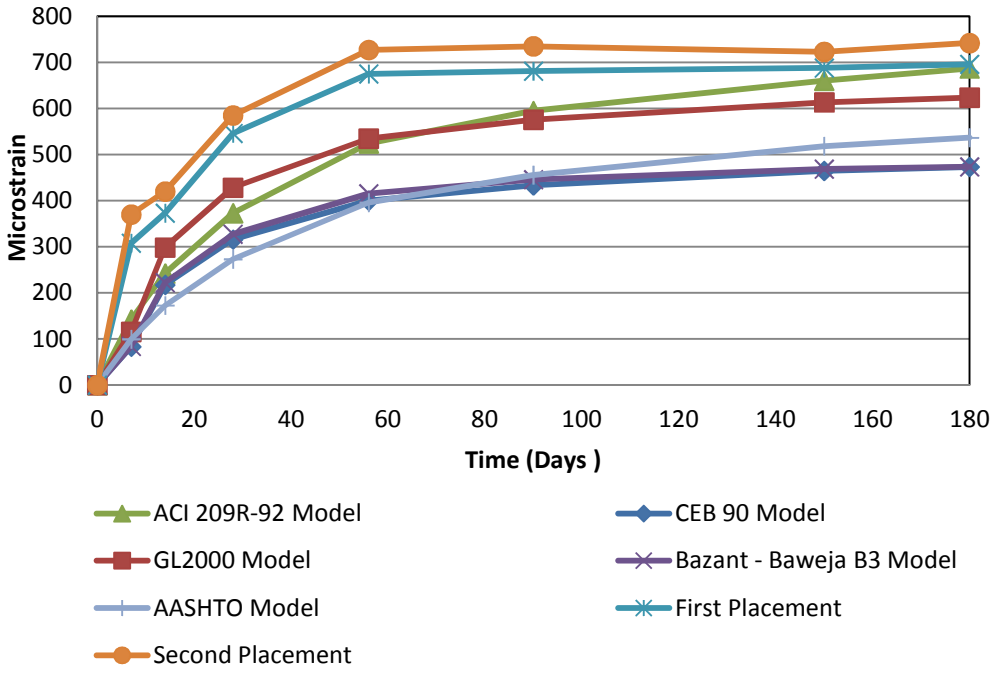

Figure 40. Shrinkage Models Comparison for 50% Relative Humidity Ponding Observations

Ponding tests were performed for the closure pour joints on each of the three lab cast slabs seven months after casting the closure pour. Water was ponded for 24 hours over each slab. After six hours, signs of water were noticed at the bottom of the closure pour joints at Slab C followed by Slab A and Slab B 20 minutes later. The first water drops were noticed after nine hours of water ponding, the water was dripping at a very slow rate estimated at one drop per 15 minutes. The maximum noticed leaking rate was one drop per 10 minutes at Slab C joints. Slab A and B had a similar behavior and leaked at a slower rate compared to Slab C. This confirmed that the closure pour joints had opened wide enough to allow water leakage through the joint similar to the deck joints, and the slabs were considered ready for fatigue and strength testing.

CONCLUSIONS

- *Cover depths were adequate, and they provided good protection against chloride attacks, for a period of 17 years, within the closure pour but not the cracked areas.*
- *Concrete shrinkage was adequate to open the construction joint.*
- *Corrosion activity was higher closer to the construction joint for I-81 bridge deck slabs.*
- *Corrosion potentials were higher for I-81 bridge deck slabs than lab cast slabs.*
- *Corrosion current densities for I-81 bridge deck slabs were higher than lab cast slabs.*

- *Corrosion current densities were higher across the joints at the closure pour for I-81 bridge deck slabs.*

- *Chloride contents along the depth of the joint were relatively uniform for the depths of 2-4 in from the top surface of the I-81 bridge deck slabs (1.64 to 4.69 lb/yd^3).*

- *Chloride content within the closure pour was very low from 2-3.5 in (0.2 to 1.0 lb/yd^3) from the top surface of the I-81 bridge deck slabs.*

- *Epoxy adhesion was in good condition on the ECR, since it could not be peeled even after soaking the ECR for two weeks in water. Although corrosion was occurring under the epoxy coating and it lost adhesion in some places.*

- *The ACI 209R-92 was the best predictor model for drying shrinkage followed by the GL2000.*

RECOMMENDATIONS

1. *VDOT's Structure and Bridge Division should conduct frequent inspections and closely monitor bridges with similar construction joint details at least every two years.* This includes visually checking leaking joints for deposits and rust stains. It also includes, measuring corrosion current densities for the reinforcing steel at different locations on the bridge deck.

2. *VDOT's Structure and Bridge Division should specify corrosion resistant reinforcement, such as stainless steel bars (ASTM A955 or ASTM A1035), for any reinforcement crossing cold joints, such as in the joint between the closure pour and the previously cast bridge deck studied in this project.*

3. *VDOT's Structure and Bridge Division should always detail shear keys at cold joints.* However, the construction of shear keys at the joint between the closure pour and the previously cast bridge deck studied in this project is not practical. Alternatively, joints should be located where there is structural support on each side.

4. *VDOT's Structure and Bridge Division should seal construction joints with flexible sealants to prevent chlorides from attacking the reinforcing steel.*

BENEFITS AND IMPLEMENTATION PROSPECTS

This study has revealed the susceptibility of smooth-faced construction joints between phases of deck construction to shrinkage cracking and subsequent reinforcing bar corrosion. The lab cast specimens were monitored for shrinkage strains and joint cracking, and indicated that cracking and leaking of the joints occurred prior to 70 days following the placement of the

closure pour concrete. This cracking allowed leaking of water and deleterious substances, which resulted in premature corrosion of the reinforcing steel crossing the joint.

The design recommendations are to use shear keys and corrosion resistant reinforcement in future construction joint details. The implementation of these recommendations should result in more durable and long lasting bridge decks built with staged construction.

The inspection and maintenance recommendations are to inspect joints carefully for leaking and seal joints to prevent ingress of corrosion inducing substances. The implementation of these recommendations should prevent future failures of previously constructed decks with similar details.

ACKNOWLEDGMENTS

The authors gratefully acknowledge the guidance and assistance provided by Michael Sprinkel at the Virginia Center for Transportation Innovation and Research. The assistance of David Mokarem, Abhilasha Maurya, Brett Farmer, and Dennis Huffman in the Murray Structural Engineering Lab at Virginia Tech was also very valuable and is gratefully acknowledged. The opinions in this report are those of the authors and not necessarily those of the sponsor.

REFERENCES

AASHTO. *AASHTO LRFD Bridge Design Specifications, 4th Edition*. American Association of State Highway and Transportation Officials, Washington, DC, 2007.

ACI Committee 224. *Control of Cracking in Concrete Structures* (ACI 224R-01), American Concrete Institute, Farmington Hills, MI, 2001.

ACI Committee 209. *Guide for Modeling and Calculating Shrinkage and Creep in Hardened Concrete* (ACI 209.2R-08). American Concrete Institute, Farmington Hills, MI, 2008

Aitcin, P.C., Neville, A.M., and Acker, P. Integrated view of shrinkage deformation. *Concrete International,* Vol. 19, No. 9, 1997, pp. 35-41.

ASTM C876-91. C876-91, Standard test method for half cell potentials of uncoated reinforced steel in concrete. *Annual Book of ASTM Standard 4*.

Balakumaran, S. S. G.. *Influence of Bridge Deck Concrete Parameters on the Reinforcing Steel Corrosion.* PhD dissertation, Virginia Polytechnic Institute and State University, Blacksburg, 2010.

Broomfield, J. P. *Corrosion of steel in concrete : understanding, investigation and repair.* Taylor & Francis, London & New York, 2007.

Brown, M. C. *Corrosion Protection Service Life of Epoxy Coated Reinforcing Steel in Virginia Bridge Decks.* PhD dissertation, Virginia Polytechnic Institute and State University, Blacksburg, 2002.

Brown, M. C., Weyers, R.E., and Sprinkel, M.M. Service life extension of Virginia bridge decks afforded by epoxy-coated reinforcement. in ASTM Symposium on Bars, *ACI Materials Journal*, Vol. 97, No. 2, 2003, pp 214-220.

Clear, K. C. Measuring rate of corrosion of steel in field concrete structures. *Transportation Research Record*, No. 1211, 1989, pp. 28-37.

Clear, K. C. Test procedures, data analysis, and general information. *3-LP Package*. K.C.C. Inc. Sterling, VA., 1990.

Feliu, S., Andrade, C., Gonzalez, J.A., and Alonso, C. A new method for in-situ measurement of electrical resistivity of reinforced concrete. *Materials and Structures,* Vol 29, No. 6, 1996, pp. 362-365.

FHWA. Retrieved 4th February, 2011, from http://www.fhwa.dot.gov/bridge/nbi/defbr10.cfm.

Grantham, M. G., Herts, B., and Broomfield, J. The use of linear polarisation corrosion rate measurements in aiding rehabilitation options for the deck slabs of a reinforced concrete underground car park. *Construction and Building Materials,* Vol. 11, No. 4, 1997, pp. 215-224.

Holt, E. and Leivo, M. Cracking risks associated with early age shrinkage. *Cement and Concrete Composites*, Vol 26, No. 5, 2004, pp. 521-530.

Liu, Y. and Weyers, R.E. Comparison of guarded and unguarded linear polarization CCD devices with weight loss measurements. *Cement and Concrete Research*, Vol 33, No. 7, 2003, pp. 1093-1101.

Mehta, P. K. and Monteiro, P. J. M. *Concrete : microstructure, properties, and materials*. McGraw-Hill, New York, 2006.

Polder, R., Andrade, C., Elsener, B., Vennesland, O., Gulikers, J., Weidert, R., and Raupach, M. Test methods for on site measurement of resistivity of concrete. *Materials and Structures*, Vol 33, No. 10, 2000, pp. 603-611.

Weyers, R., Pyc, W., Sprinkel, M.M., and Kirkpatrick, T.J. Bridge deck cover specifications. *Concrete International*, Vol 25. No. 2, 2003, pp. 61-64.

APPENDIX

DECK SLABS SKETCHES AND CUT LOCATIONS

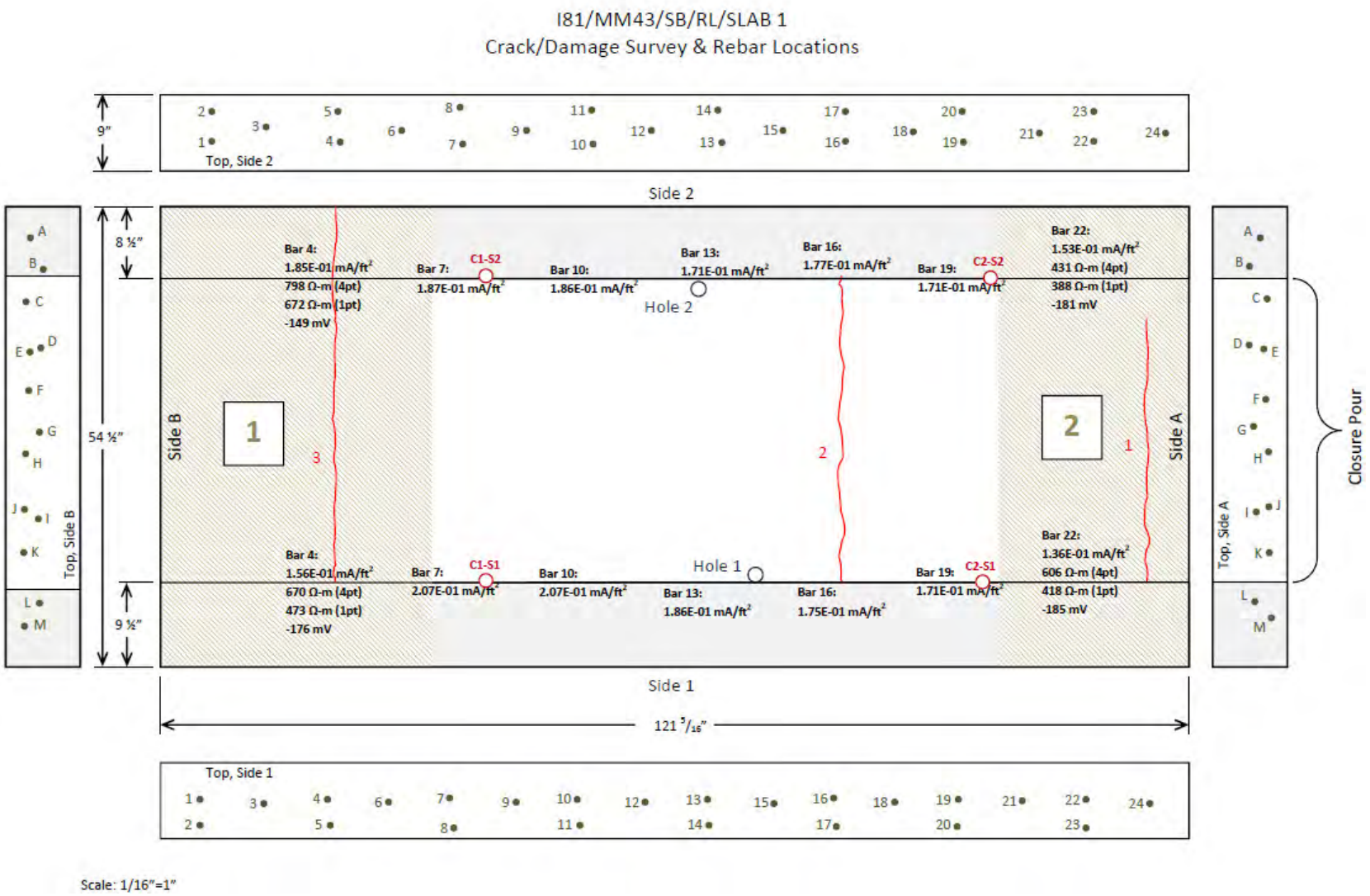

Figure A.1. Crack, Damage Survey and Rebar Locations for Slab 1

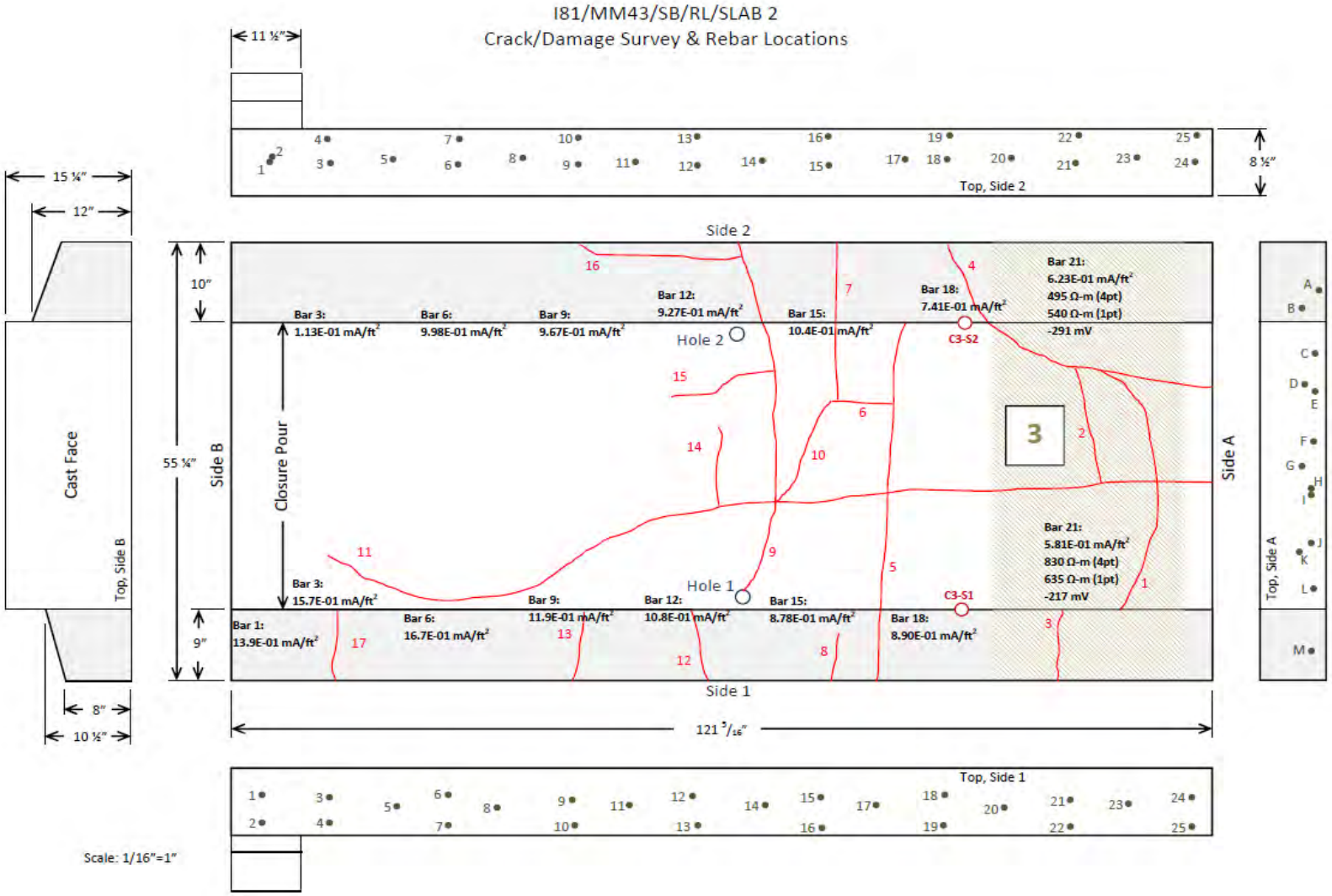

Figure A.2. Crack, Damage Survey, and Rebar Locations for Slab 2

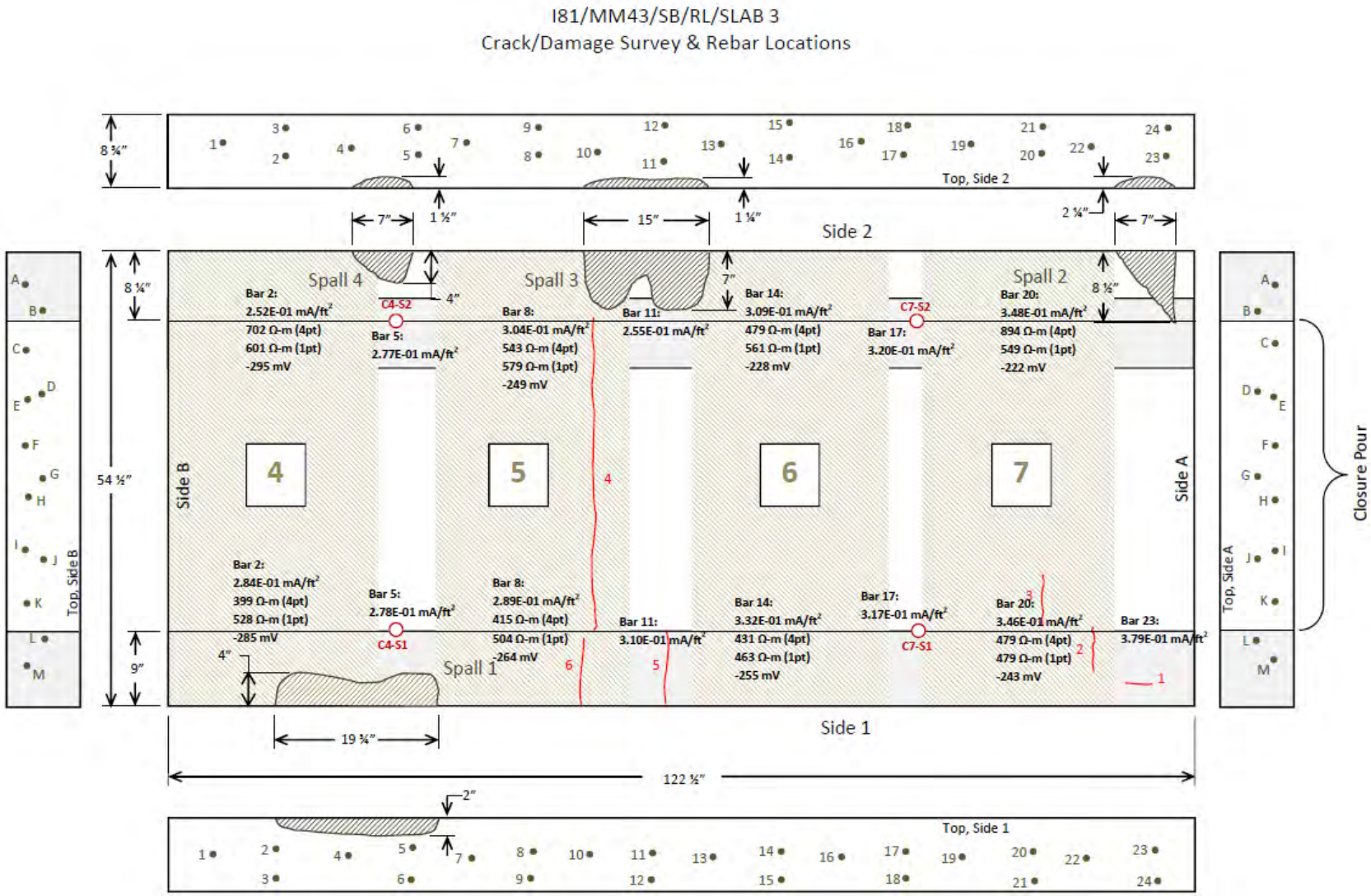

Figure A.3. Crack, Damage Survey, and Rebar Locations for Slab 3

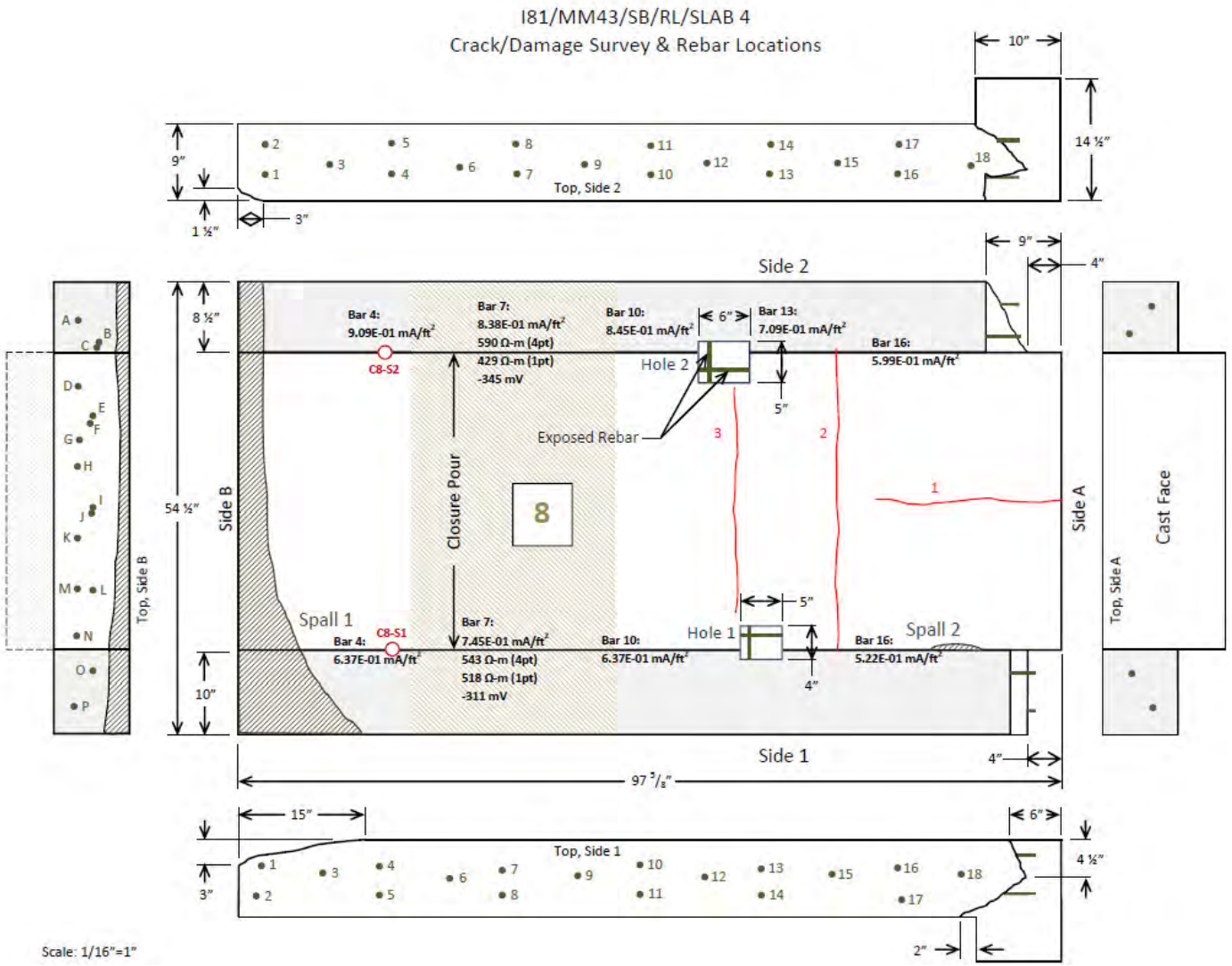

Figure A.4. Crack, Damage Survey, and Rebar Locations for Slab 4